Fifth Annual Translational Research Symposium

"In Memory of David C. Seldin, MD, PhD (1957-2015)"

March 28, 2016

Poster Presentations

This year's poster session incorporated 57 ePoster board presentations illustrating a broad range of translational science topics. All trainee posters were judged on eight different criteria, resulting in four posters receiving a top score and a $1,000 prize. The four winners are listed below, followed by abstracts of the posters presented at the symposium. Congratulations to the winners and to all the participants.

POSTER SESSION WINNERS

#4: *"Degradation of Gliadins in the Gastro-intestinal Tract of Mice"* (p 3-4) - **Ghassan Darwish**

#12: *"Fetal Hemoglobin Regulation in Sickle Cell Anemia"* (p 9-10) - **Elmutaz M. Shaikho**

#24: *"Disposable Cartridge Platform for Rapid Multiplex Detection of Viral Hemorrhagic Pathogens from Plasma and Whole Blood"* (p 20-21) - **Steven M. Scherr**

#30: *"PDGFRβ Is a Novel Marker of Stromal Activation in Oral Squamous Cell Carcinomas"* (p25-26) - **Vinay K. Kartha**

1. **Predicting Lung Function Decline in COPD using Bronchial Airway Gene Expression**
   Katrina Steiling, Elizabeth Becker, Gang Liu, Xiaohui Zhang, Yuriy O Alekseyev, Stephen Lam, Maarten van den Berge, Avrum Spira, Marc E Lenburg,

Background: Chronic Obstructive Pulmonary Disease (COPD) is the third leading cause of death, and is characterized by variable but progressive lung function decline. The mechanisms underlying this progression are not well understood. Given our recent description of a bronchial airway gene expression signature associated with COPD and lung function impairment, we sought to identify a signature that predicts rapid lung function decline in individuals with COPD.

Methods: We previously generated a dataset consisting of bronchial airway brushings from patients with COPD(n=87) measured on Affymetrix Human Gene 1.0 ST microarrays. From this dataset we selected the samples from 54 individuals who had at least one additional spirometry measurement performed $\geq$4 years subsequent to sample collection. Bronchial airway gene-patterns that at baseline were associated with subsequent decline in FEV1 were identified using a linear model with ANOVA controlling for relevant co-variates. Enriched pathways and biologic functions were identified using GATHER. GSEA was used to evaluate the relationship between gene-expression patterns significantly associated with lung function decline and the COPD signature, and with dataset of subjects with COPD treated with fluticasone.

Results: A total of 268 genes were significantly associated with FEV1 decline among individuals with COPD (FDR<0.25). Genes whose expression associated with alterations in lung function were significantly enriched in immune response and ubiquitin cycle ($p<0.05$). The genes associated with lung function decline in COPD patients were also associated with an airway gene-expression signature of the presence or absence of COPD (GSEA-FDR<0.01), and enriched for genes that are reversed by fluticasone (GSEA-FDR<0.01).

Conclusion: We have identified a gene expression signature that is associated with future FEV1 decline in participants with COPD. This signature might have utility as a biomarker to stratify patients for clinical trials of anti-COPD therapies, a surrogate biomarker of therapeutic efficacy, or predictor of COPD development.

2. **Request Not to Publish**

3. **The sst1 locus controls TNFa-induced stress response to limit immunopathology**
   Bidisha Bhattacharya[1], Sujoy Chatterjee[1], Robert Berland[2] and Igor Kramnik[1]

Emergence and spread of drug resistant forms of *Mycobacterium tuberculosis* calls for the development of novel host-directed therapies (HDTs). Revealing mechanisms controlling

progression and necrotization of TB granulomas in the lungs allows the development of pathogenesis-oriented therapies targeting lung damage induced by Mtb. Using forward genetic analysis in a mouse model of tuberculosis we identified a genetic locus sst1 that specifically controls necrotization within TB granulomas. An interferon-inducible nuclear protein IPR1 within the sst1 locus was identified by positional cloning. We determined that the sst1/IPR1-mediated pathway is involved in control of macrophage responses to TNFa. The IPR1 protein was detected in the nuclei of the B6 macrophages within 12 hours after stimulation with 10 ng/ml of TNFa, but it was not expressed in congenic macrophages that carried the sst1 susceptible allele (B6-sst1^S). We used whole genome expression profiling (RNA-seq and Affymetrix GeneChip microarray analyses) to compare the effect of TNFα on sst1 resistant (IPR1-positive) and sst1-susceptible (IPR1-negative) macrophages in vitro. The sst1^S macrophages displayed upregulation of interferon-beta (IFNb) and integrated stress response and down regulation of metabolic pathways. At 18 - 24 hours they remained viable, but entered a pro-apoptotic state (PAS) characterized by high levels of expression of genes involved in apoptosis and died more readily after subsequent infection with intracellular bacteria. Transition to PAS required continuous TNFa and JNK signaling, as well as IFN-I and ROS production and PKR induction, but was NF-kB-independent. We concluded that the *sst1/IPR1* locus encodes a protective switch activated by continuous stimulation with TNFa, acting via negative regulation of JNK, type I IFN and PKR. This mechanism, as well as pathways predominantly activated by TNFa in IPR1-deficient cells and leading to their demise, represent promising targets for host-directed therapies aimed at preventing macrophage death and reducing TNF-mediated pathology in chronic inflammatory conditions.

4. **Degradation of gliadins in the gastro-intestinal tract of mice**
   Ghassan Darwish, Chin-Hua Yang, Na Tian, Guoxian Wei, Eva J. Helmerhorst

Introduction: Celiac disease is a chronic immune-mediated inflammation of the duodenum, triggered by gluten contained in wheat, barley and rye. Our previous studies have shown that Rothia, Gram-positive oral bacteria, have the ability to degrade and detoxify gluten in vitro. The objective of this study was to test if R. aeria bacteria can degrade gluten that is naturally contained in mice food in vitro and in vivo. Methods. Gluten digestion in vitro was monitored in mice chow with and without added R. aeria bacteria (OD620 200 per 1 g of chow) after 0, 2 and 4h incubation. For the in vivo experiment, two balb/c mice were fed with chow with and without added R. aeria bacteria and sacrificed after 2 h. The stomach, duodenum, jejunum and ileum contents were harvested and gluten degradation was assessed by SDS PAGE and immunoblotting, and with the G12 ELISA assay detecting immunogenic gluten epitopes. Results. In vitro, gliadins were stable in food incubated in the absence of R. aeria, but degraded within 2h in the presence of R. aeria. In vivo, fasted mice readily consumed the 1 g food without or

with the added bacteria. After 2h, the distribution of the chyme in the stomach and the small intestines was determined to be approximately 64%/36%. Gliadins were detected by immunoblotting in the stomach, but not in the small intestinal samples, of both the control and the R. aeria-fed mice. G12 ELISA results provided preliminary evidence that gluten epitopes in the duodenum, jejunum and ileum of R. aeria-fed mice were reduced as compared to the control mice. Conclusion. These pilot study results provide the basis for further investigation to fully establish the extent to which R. aeria can digest and abolish immunogenic gluten epitopes in vivo. Supported by NIH/NIAID grants AI087803 and AI101067.

5. **Chamber-specific dysregulation of genes in MEF2A-deficient hearts**
   Jose L. Medrano (Trainee); Co-Author: Dr. Francisco J. Naya (Lab Principle Investigator)

Proper regulation of the pathways expressed in the mammalian heart involves a complex spatiotemporal pattern of signaling and gene expression. Perturbations in this gene regulatory network can lead to severe congenital heart defects, cardiac failure, and death. The myocyte enhancer factor 2 (MEF2) family of transcription factors are key regulators of both muscle-specific and ubiquitous cellular pathways. Although the four mammalian MEF2 isoforms, designated MEF2A, -B, -C, and -D, are coexpressed in cardiac muscle, targeted inactivation of each specific isoform reveals dramatically different cardiac phenotypes suggesting distinct in vivo functions.

To identify the chamber-specific functions of MEF2A and uncover the defective cellular and molecular gene programs in the adult knockout (KO) heart, I performed an initial microarray screen by separately isolating total RNA from atrial and ventricular chambers of both wild type and Mef2a KO mice (n=7). Subsequently, differences in gene expression between knockout and wild type atria, and knockout and wild type ventricles were analyzed via microarray analysis. A total of 686 genes (atria and ventricles) were dysregulated by at least 1.5-fold in Mef2a KO hearts. Of the total dysregulated genes, 481 genes were preferentially dysregulated in KO atria, 158 genes were preferentially dysregulated in KO ventricles, and the remaining 47 genes were dysregulated in both KO atria and ventricles.

In an effort to understand the spatial gene dysregulation pattern in Mef2a KO hearts, we hypothesized that MEF2A interacts with a different cohort of cofactors in the cardiac chambers to regulate its target genes. Therefore, we computationally analyzed the promoter regions of atrial and ventricular dysregulated genes to identify candidate transcription factor binding sites which may cooperate with MEF2A. A better understanding of the genes and pathways dysregulated in the adult Mef2a KO hearts will provide insight into the molecular mechanisms of region-specific cardiomyocyte function in the mammalian heart.

6. **Expression of the Novel Cell Adhesion Molecule TMIGD1 in Human Trophoblast Cells**

Cynthia Wang*1, Jeffrey Pudney1, Rosana D Meyer2, Philip A Bondzie2, Xueqing Zou2, Nader Rahimi2 and Wendy Kuohung1

Introduction: Transmembrane and immunoglobulin domain-containing 1 (TMIGD1) is a newly identified cell adhesion molecule that mediates cell-cell interactions and is mainly expressed in the kidney and colon. In renal epithelial cells, TMIGD1 regulates cell proliferation and migration. TMIGD1 expression was also found to be downregulated in human colon tumors. Human tissue panels showed expression of TMIGD1 in placenta. Given previous evidence that placental invasion shares certain characteristics with tumor metastasis, we elected to study the expression and function of TMIGD1 during placentation. This is of interest because dysregulation of placental invasion may lead to obstetrical complications such as preeclampsia and intrauterine growth restriction (IUGR). We hypothesize that TMIGD1 is expressed in trophoblast cells and regulates cell migration during placental invasion.
Methods: Placental samples were collected at the time of elective pregnancy terminations under an IRB-approved protocol. TMIGD1 localization in trophoblast was visualized using immunofluorescence (IF). We overexpressed TMIGD1 in the immortalized trophoblast cell line HTR8/SVneo using a retroviral vector. Transfection was verified using IF, Western blot, and qPCR to compare the modified and original cell lines. The migration of TMIGD1 overexpressing HTR8/SVneo cells was assessed using a wound-healing assay and a transwell migration assay. Unpaired t-tests were used for data analysis.

Results: We observed TMIGD1 localization in the apical region of syncytiotrophoblasts. TMIGD1 mRNA expression in our transfected HTR8/SVneo cells was 3-fold greater than that in the original line, and 400-fold greater in first trimester whole placenta. Compared to the untransfected HTR8/SVneo cells, the TMIGD1 overexpressing cells exhibited a 30±5% decrease in migration in our wound-healing assay. In transwell assays, TMIGD1 overexpression suppressed migration by 55%, compared to control cells.

Conclusion: Our findings show for the first time that TMIGD1 is expressed in trophoblast cells and exhibits an inhibitory role in cell migration. This evidence supports the idea that TMIGD1 may serve an important function in regulating placental invasion.

7. **Novel compound(s) for host directed therapy (HDT) of intracellular bacterial infections**

Sujoy Chatterjee[1], Bidisha Bhattacharya[1], William G. Devine[2], Lester Kobzik[3]
Aaron B. Beeler[2], John A. Porco, Jr.[2] and Igor Kramnik[1]

Drug-resistant bacteria represent a significant global threat. Given the dearth of new antibiotics, host-directed therapies (HDTs) are especially desirable. As IFN-gamma (IFNγ) plays a

central role in host resistance to intracellular bacteria, including Mycobacterium tuberculosis, we searched for small molecules to augment the IFNγ response in macrophages. Using an interferon-inducible nuclear protein Ipr1 as a biomarker of macrophage activation, we performed a high-throughput screen and identified molecules that synergized with low concentration of IFNγ. Several active compounds belonged to the flavagline (rocaglate) family. In primary macrophages they 1) synergized with low concentrations of IFNγ in stimulating expression of a subset of IFN-inducible genes, including a key regulator of the IFNγ network, Irf1; 2) suppressed the expression of inducible nitric oxide synthase and type I IFN and 3) induced autophagy. We further screened a sublibrary of 69 rocaglate derivatives prepared at BU-CMLD (Director John Porco). After evaluation for Irf1 expression, toxicity, and activation of primary macrophages, we identified the aromatic ketones as the most promising leads. We subsequently synthesized and assayed the single enantiomer of our best candidate, which was significantly more potent, verifying that absolute stereochemistry is critical for efficient interaction with the target. Interestingly we have identified an IFN independent property of rocaglates to induce expression of prostaglandin-endoperoxide synthase 2 (Ptgs2/Cox-2), which is regulated by activation of stress kinase p38 pathways. In addition our results show that rocaglates retain their unique property of macrophage activation in B6-sst1S (B6-sst1 susceptible mice) where loss of genetic locus sst1 from B6 resulted inflammatory tissue damage after bacterial infection and necrotization of TB granulomas. Taken together we argue that rocaglates serve a potential candidate for novel HDTs especially relevant to fighting drug-resistant pathogens, where improving host immunity may prove to be the ultimate resource.

8. **Search for genetic modifiers that up-regulate fetal hemoglobin expression in asymptomatic β^0-thalassemia homozygotes**
   Zhihua Jiang, Hong-yuan Luo, John J. Farrell, Martin H. Steinberg, David H.K. Chui

Background: Beta-thalassemia is among man's most common monogenic diseases. The mutation renders the affected β-globin gene incapable of producing β-globin chains. Most β^0-thalassemia homozygotes are severely anemic and require monthly blood transfusions.

Objective: To understand the genetic basis of transfusion-independent β^0-thalassemia homozygotes.

Hypothesis: We hypothesize that inherited rare mutation(s) allow the synthesis of large amounts of HbF ($\alpha_2\gamma_2$) to supplant the lack of HbA ($\alpha_2\beta_2$).

Methods and Results: Two dizygotic twin young men were homozygous for β^0-thalassemia mutation [2-nucleotide-deletion in codon 8 which results in frame-shift]. Yet they were well and never transfused *(Jiang et al, Brit. J. Haematol. Jan. 2016).* Their Hb was 12-13 g/dL, 97% of

which was fetal hemoglobin (HbF). We also studied 22 other patients homozygous for the same β^0-thalassemia mutation. All were severely anemic and transfusion dependent.

There are 3 known major HbF quantitative trait loci on Chr. 2, 6, and 11. Together, they account for 20-50% of HbF variance in different populations. The twins were homozygous for the QTL on Chr. 6q23, 3-bp deletion in the *HBS1L-MYB* intergenic region *(Farrell et al, Blood 117: 4935, 2011),* which was not found in any of the other 22 patients.

In anticipation of full scale genomic and functional studies, whole genome sequencing was done on one twin and two severe patients. Variants found in the twin after filtering with the following metrics were: 1) quality control, 4,322,744; 2) minor allele frequency <0.01, 661,366; 3) subtract variants found in the 2 severe patients, 197,137; 4) coding variants, 1,096; 5) non-synonymous variants, et al, 667; 6) SIFT score <0.05, 324; 7) homozygous variants, 19; 8) significant expression in human CD34+ derived erythroid cell culture, 6.

Significance: Novel genetic modifier(s) that up-regulate HbF expression discovered in these patients could have implications for therapeutics to treat β-thalassemia and sickle cell di Abstract contact name: Gloria Chan

9. **Proteomic blood profiling in transthyretin-associated forms of amyloidosis**
Gloria G Chan[1] ; Lawreen H Connors[1,2]

Introduction: The amyloidoses are a collection of fatal protein misfolding diseases which include forms associated with the plasma protein, transthyretin (TTR). Referred to as the ATTR amyloidosis to reflect the biochemical nature of the amyloid, these diseases frequently feature extracellular deposits of TTR in heart and nerve tissues. Both wild-type and mutant forms of TTR are amyloidogenic and responsible for organ and tissue damage in ATTRwt (acquired) and ATTRm (inherited) forms, respectively. An accurate diagnosis of ATTR amyloidosis can be challenging, as biopsy evidence usually from the affected tissue is required. Thus, the discovery of biomarkers that signal onset and progression of amyloid disease could potentially improve diagnosis and reveal key information regarding disease mechanisms. The aim of this study was to investigate serum proteomic identifiers in ATTR amyloidosis.

Methods: Sera were selected from patients with ATTRwt or ATTRm, and controls; samples containing equivalent amounts of serum from 10 cases in each of the 3 groups were pooled and studied. Patient and control groups were age-, gender-, and race-matched. Characteristics of ATTRm include cardiomyopathy (CMP) or polyneuropathy (PN). The proteomic analyses were performed using PeptiQuant™ Human Discovery Assay (MRM Proteomics) to determine the presence and relative protein concentrations of 192 human proteins in the samples. Welch t-test for unequal variance was performed and adjusted using the false discovery rate (FDR) test; values of $p < 0.05$ indicated significant differences. Comparisons between ATTRwt *vs.* ATTRm and ATTRm-CMP *vs.* ATTRm-PN were further analyzed using STRING and DAVID databases to predict protein-protein interactions and identify gene functional and annotation clustering.

Results: Initial comparison of patient and control groups showed significant differences in serum levels of 123 proteins. ATTRwt *vs.* ATTRm comparison showed 6 unique proteins (e.g. transthyretin) and ATTRm-CMP *vs.* ATTM-PN showed 19 unique proteins (e.g. fibulin-1 and beta-2-microglobulin), predicting two independent protein-protein interaction networks by STRING. Some enriched functional annotation terms from the comparisons in DAVID include disulfide bond, signal, extracellular matrix, complement and coagulation cascades, disease mutation, and response to wounding.

Conclusions: Our results show significant differences in the serum proteomes of ATTR and control serum. Protein concentrations, interactions, and functions that were unique to ATTRwt, ATTRm-CMP, and ATTRm-PN were identified.

10. **Transthyretin (TTR) and retinol-binding protein (RBP4) are predictors of survival in wild-type transthyretin amyloidosis (ATTRwt)**

    Abstract primary author: Jacquelyn LS Hanson1,2; Abstract co-authors: Clarissa M Koch1,2, Gloria G Chan1, Lawreen H Connors1,2

Introduction: ATTRwt is a poorly understood sporadic cardiomyopathy primarily diagnosed in elderly Caucasian men with an undefined pathogenesis and no validated biomarkers. Our objective was to identify ATTRwt-specific diagnostic and prognostic indicators. Since serum TTR levels are low in ATTRm, and possibly in ATTRwt, we predicted that TTR and its binding partner, RBP4, could serve as ATTRwt-specific markers.

Methods: ATTRwt and ATTRm subjects were males over age 60 with cardiac involvement. Healthy controls were Caucasian males over age 60. Clinical and laboratory data were obtained from the BU Amyloidosis Center IRB-approved clinical database. Serum TTR concentrations were determined by immunoturbidity assay in the Boston Medical Center Pathology Laboratory. Serum RBP4 levels were determined by ELISA developed in our laboratory. Correlations between laboratory parameters and TTR or RBP4 were determined by Pearson or Spearman tests, depending on normality via the Shapiro-Wilk test. Cox univariate and multivariate survival, ROC curves, and cut-offs were determined.

Results: Compared to controls, serum TTR was lower in ATTRm ($p < 0.0001$) and slightly lower in ATTRwt, though not significantly. RBP4 concentrations were increased in ATTRwt compared to ATTRm ($p = 0.0014$) and controls ($p < 0.0001$). In ATTRwt, TTR was uniquely correlated with BNP ($r = -0.212$, $p = 0.036$) and low TTR was associated with arrhythmia ($p = 0.0051$). Further, RBP4 was uniquely correlated with cTn-I ($r = 0.225$, $p = 0.026$) and IVST ($r = 0.203$, $p = 0.046$) in ATTRwt. Unique predictors of survival in ATTRwt were RBP4 ($p = 0.016$), cTn-I ($p < 0.0001$), and uric acid ($p = 0.0075$). At one-year follow-up, treated subjects had higher TTR ($p = 0.0001$) than untreated,

corresponding to measurable disease improvement, lower BNP (p =0.043) and higher LVEF (p =0.040).

Conclusions: TTR and RBP4 are unique ATTRwt markers of disease status, as low TTR and high RBP4 are uniquely associated with markers of worsening disease and predictors of survival.

11. Characterization of a Transcript Found Within the HBS1L-MYB Intergenic Region

Tasha A. Morrison*, Ibi Wilcox, Hong-Yuan Luo, Martin H. Steinberg and David H.K. Chui.

The HBS1L-MYB intergenic region on chr6q23 is important for the regulation of erythroid proliferation/maturation and hemoglobin expression. Discovered in this region are single nucleotide polymorphisms (SNPs) that are associated with high fetal hemoglobin (HbF)—this hemoglobin is beneficial to patients with hemoglobinopathies—and an enhancer that regulates expression of the downstream gene MYB. Based on previous findings of transcription within the HBS1L-MYB intergenic region, we set out to characterize the transcript and determine if it is a long noncoding RNA (lncRNA) that functions to regulate MYB expression, erythroid proliferation/maturation and hemoglobin expression. Using cDNA from K562 cells, we were able to amplify by PCR a fragment greater than 1 kb. Next, 5'- and 3'-RACE reactions were done to determine the full length of this transcript. These results were also confirmed in primary erythroid cells derived from cord blood CD34+ cells. It is known that lncRNAs display differential expression during development and tend to be tissue-specific. Therefore, we looked at expression of this transcript during differentiation of primary erythroid progenitors cells, and found that its expression modulates during this process. We also found that this transcript is tissue-specific—expressed mostly in tissue of hematopoietic origin. Further analyses are underway to determine its function. This novel transcript is a candidate for being a lncRNA. Since this fragment is transcribed from a region known to be associated with HbF variability and regulate MYB expression, it will be of interest to determine its role as it relates to erythroid differentiation and hemoglobin expression.

12. Fetal Hemoglobin Regulation in Sickle Cell Anemia

Elmutaz M. Shaiko1; Co-authors: Alawi H. Habara1, Abdulrahman Alsultan2, A.M. Al-Rubaish3, Fahad Al-Muhanna3, Z. Naserullah4, A. Alsuliman5, P.K. Patra6, Paola Sebastiani7, Kristin Baltrusaitis7, John J. Farrell1 , Zhihua Jiang1, Hong-yuan Luo1, Jacqueline N. Milton7, George Murphy1, Gustavo Mostoslavsky1, David. H.K. Chui1, Amein K. Al-Ali8, Martin H. Steinberg1

Background: Fetal hemoglobin (HbF) modulates the phenotype of sickle cell anemia; inducing high levels is therapeutically beneficial. Hypothesis: A full understanding the genetic basis of

high HbF regulation has prognostic and potential therapeutic value. Objectives Examine the genetic basis of HF variability in the Arab-Indian (AI) β-globin gene cluster haplotype of sickle cell anemia where the disease is milder because HbF levels are higher. Methods: Genome-wide association studies, whole genome sequencing, exome sequencing, RNA sequencing and disease modeling in induced pluripotent stem cells (iPSCs) were used to identify genetic variants associated with HbF in sickle cell anemia patients of diverse ethnicities. Results: BCL11A, MYB and a locus linked to HBB were associated with HbF. Homozygosity for a T/C/T/A/T haplotype of rs16912979 (HBB locus control region (LCR), rs7119428 and rs97336333 (ZBTB7A binding sites in the LCR) and rs7482144 and rs10128556 (5" to HBG2 and in HBBP1) was exclusive to the AI haplotype and was associated with H3K27Ac marks, DNase hypersensitivity, GATA1 and TAL1 binding. The functional elements of this haplotype might be required for optimally functional looping of the LCR to the HBG2 promoter enhancing its transcription compared with that of HBB. Two intronic SNPs in ANTXR1, rs4527238 and rs35685045, were associated with HbF only in AI haplotype cases and alone accounted for 10% of the HbF variability; with BCL11A, about 15% of HbF variability was explained. ANTXR1 was expressed in erythroid progenitors derived from iPSCs and from CD34+ cells. As CD34+ cells matured to erythroid cells, HbF fell and ANTXR1 expression increased; the opposite pattern accompanied iPSC differentiation to erythroid progenitors. ANTXR1 might affect HbF regulation indirectly through Wnt signaling and directly by modulating histone deacetylase and HbF gene expression.Conclusions: Novel genetic elements, with other HbF modulators, might have prognostic value; if validated mechanistically they could be potential therapeutic targets.

13. **Radiation Exposure Induces Alterations Typical of Oxidative Stress Modifications Underlying Cardiovascular Disease**
    Mark E. McComb, Stephen A. Whelan; Chunxiang Yao; Jean L. Spencer; Christian Heckendorf; Dan Berkowitz; Maggie Kuo; Catherine E. Costello; Markus M. Bachschmid

Introduction: There is renewed interest in space exploration, including travel to the moon and Mars. Apart from a catastrophic event, a major risk to astronauts is prolonged exposure to Galactic Cosmic Radiation. Radiation exposure results in increased free radicals at the cellular level, which can cause DNA and protein damage, metabolic oxidative stress and formation of oxidative post-translational modifications on proteins. In addition to increased likelihood of cancer, prolonged exposure heightens the risk of cardiovascular disease (CVD). Building upon our studies of metabolic syndrome induced CVD, we used a mouse model of radiation exposure as a first stage to identify protein and PTM changes associated with exposure to radiation, altered redox biology, and their impact on cell injury and CVD.

Methods: Mice were exposed to 1 GeV Fe ions at 0.5 Gy/min at doses of 0 Gy, 0.5 Gy and 5 Gy. Heart tissue samples were collected from the mice, prepared using standard procedures, and

tryptic peptides were subjected to proteomics analyses. LC-MS/MS was carried out on a Q Exactive MS coupled with a Waters NanoAcquity HPLC. Label-free quantification was conducted using both Scaffold (Proteome Software)and Progenesis LCMS (Nonlinear Dynamics). MS/MS data were processed using Proteome Discoverer (Thermo-Fisher) and Mascot (Matrix Science) software, searching custom protein and post-translational modification (PTM) databases. Collation and meta-analysis were conducted using the Trans Proteomic Pipeline (ISB), Scaffold and STRAP PTM (in-house) software. Ingenuity Pathway Analysis (IPA, QIAGEN) was used to identify dose-dependent biological pathways.

Results: Label-free analysis identified more than 51,000 total peptide features with approximately 3,600 features changing as a function of dose (p=0.05 ANOVA). Of these, more than 1,900 were identified via MS/MS (p=0.05 FDR). Approximately half of the peptides which were observed to change were in fact posttranslationally modified. Principal component analysis (PCA) and agglomerative hierarchical clustering (AHC) showed groupings of changes which were dose-dependent. Select groups were analyzed with IPA and indicated dose-dependent pathway-specific changes including CVD related pathways: Post-Translational Modification, Energy Production, Lipid Metabolism, Free Radical Scavenging, Cardiovascular Development and Function and Metabolic Disease. Several known markers of cardiovascular disease were observed to change with dose. For example, we observed an increase in Troponin I. Troponin I expression changes are related with cardiomyopathy, ventricle hypertrophy and dilation and reduced diastolic volume. In addition to CVD markers, we observed PTM changes on proteins related to cardiac function and metabolism. Mapping of PTMs indicated that both site- and region-specific changes are observed and that these changes correlate well to sensitive sites of modification observed in our other mouse and human models of CVD.

Discovery of potential biomarkers: peptide, proteins, PTMs will allow us to gain insight into the etiology of CVD, understand host physiological response to pathogenesis and afford earlier detection, improve diagnosis and treatment.

14. Top-down MS/MS Hemoglobinopathy Screening of Neonatal Samples

Roger Théberge1, Carolyn Hoppe2, Christian Heckendorf1, Cheng Lin1, David H. K. Chui3, Catherine E. Costello1, Mark E. McComb1

Introduction: More than 1200 recognized hemoglobin structural variants exist in the human population, and many of these underlie phenotypic diseases. Mass spectrometry constitutes a rapid and accurate means for the detection and characterization of Hb variants. In previous work, we demonstrated the ability of MALDI-ISD (in-source decay) on a TOF/TOF instrument to detect and characterize clinically important Hb variants residing in the N-terminal region of the

beta chain (sickle cell, Hb C and Hb E). In our continuing efforts to develop Top-down mass spectrometry-based methods to detect and characterize hemoglobin variants, we now compare results using MALDI-ISD on two different instruments (TOF/TOF and FT-ICR). The goal is to extend the scope of ISD to hemoglobin sequence variations positioned throughout globin chains.

Methods: Whole blood was obtained through screening programs from the Hemoglobin Diagnostic Reference Laboratory at Boston University School of Medicine and the hemoglobinopathy laboratory at Children's Hospital Oakland Research Institute (CHORI). The sDHB matrix solution was prepared to a concentration of 50 g/L in 50% acetonitrile/water/0.1% formic acid. A saturated solution of 1,5-DAN matrix was prepared in the same solvent mixture. Diluted whole blood was mixed with the matrix solution. MALDI-ISD mass spectra were acquired on Bruker UltrafleXtreme MALDI-TOF/TOF MS and Bruker SolariX FT-ICR MS with an actively shielded and refrigerated 12-Tesla magnet. Spectra consisted of 12,000 to 15,000 accumulated laser shots. The fragment masses were analyzed using BioTools and BUPID-Topdown (Boston University Protein Identifier-Topdown), a custom-programmed software algorithm written in-house.

Preliminary results: The MALDI-ISD mass spectrum of normal hemoglobin exhibits extensive and complex fragmentation consisting mainly of c, z and y-ions. The fragmentation roughly covers the first 70 amino acids from the N- and C-termini of normal hemoglobin. A comparison of the results obtained with the TOF/TOF and FT-ICR MS systems demonstrates that the high resolving power of the FT-ICR can be very useful to separate overlapping ISD fragment ions that are not resolved in the TOF/TOF spectra. For example, the beta c34 ion (m/z 3584.981) cannot be resolved from the alpha c34 (m/z 3585.863) and beta z33 (m/z 3584.891) product ions but these are resolved at 60,000 resolution with the FT-ICR. This experiment clearly demonstrates that the important beta marker ion c34 is the dominant component in the m/z 3584-3590 cluster. This conclusion was substantiated when a homozygous sickle cell hemoglobin sample was analyzed by MALDI-ISD FT-ICRMS. The high mass accuracy (sub-ppm) of the FT-ICR also facilitates the use of our in-house variant characterization software, BUPID. Significant differences in fragmentation were observed between the two instruments, most likely due to the higher pressure that provides vibrational cooling in the FT-ICR ion source. The observation of matrix-fragment ion adducts in the MALDI-ISD FT-ICR spectra strongly supports this correlation. A feature of MALDI-ISD TOF/TOF MS is that fragment ion signal decreases rapidly at higher m/z (>5000). We are in the process of investigating means to increase the signals from higher m/z fragment ions through a sample load study and varying matrix chemistry. Our results obtained with the FT-ICR mass analyzer suggest that the ion storage capability of that instrument could be useful for increasing ISD sensitivity for fragment ions at higher m/z.

15. **A new variant consisting of the duplication of TTR codons 71, and 72 (E51_S52dup):observed in a patient with familial amyloidotic polyneuropathy**

[1]B Spencer, [1]P Soo Hoo, [1]T Prokaeva, [1]L Connors

Background: Transthyretin amyloidosis (ATTR) is the most common form of familial amyloid (AF). More than 100 amyloidogenic mutations have been identified in transthyretin (TTR). Virtually all of the disease associated mutations reported have been amino acid substitutions. We present a new and unusual ATTR mutation identified at the Amyloidosis Research Center.

Methods: A diagnosis of AF was made by Congo red histology, and serum screening using IEF. Mutation analysis was performed by direct DNA sequencing.

Results: The patient diagnosed at out center was a 38 year old African American male. Symptoms at presentation included sensory-motor peripheral neuropathy, polyneuropathy, autonomic neuropathy, and myopathy. During the first visit, the patient reported experiencing symptoms over the course of the last twelve months. Despite treatment with diflunisal, started within three months of the diagnosis, the disease quickly progressed. In less than four years, the patient died of pneumonia, with heart failure as a secondary cause of death. Family history indicated that the father died at age 46, and the brother at 34. At diagnosis serum screening by IEF showed a variant TTR. Congo red staining of a fat biopsy was strongly positive (2-3+) for congophilic deposits. DNA sequencing of all four TTR exons showed a duplication, p.E71_S72dup (c.211_216dupGAGTCT) in exon 3. This new mutation, which increases the number of amino acid residues present in the protein TTR, from 147 to 149, has never before been reported.

Conclusion: The disease course observed in this patient suggests that the observed duplication within the TTR protein (p.E71_S72dup) causes aggressive ATTR disease.

16. **Imaging Mass Spectrometry: A Valuable Tool for Investigating Molecular Pathology of Traumatic Brain Injury**

Bo Yan1, Andrew M. Fisher2,3, Yi Pu1, Chad A. Tagge2,3, Mark E. McComb1, Lee E. Goldstein2,3,4, Catherine E. Costello1

Traumatic brain injury (TBI) is a leading cause of death and disability and is associated with increased risk of developing age-related neurodegenerative diseases, e.g., Alzheimer disease (AD) and chronic traumatic encephalopathy (CTE). However, the TBI-related pathology remains largely unknown. Here, we report results obtained using matrix-assisted laser desorption/ionization mass spectrometry (MALDI-MS) as the imaging tool to monitor multiple biomolecules in two mouse models of traumatic brain injury. Our hypothesis is that the specific information on biomolecular distributions generated by MALDI-MS imaging will provide critical insight into the pathology of TBI.

Male C57BL6 mice were subjected to impact and blast TBI according to IACUC approved protocols. MALDI imaging MS experiments were performed on a Bruker solariX 12-T FT-ICR MS and a Bruker ultrafleXtreme TOF/TOF MS.

We mapped multiple biomolecules simultaneously using MALDI-MS imaging. The observed anatomical distribution and differentiation of heme after TBI were provided a biomarker for hemorrhagic vascular disruption after TBI. The measured lipid and protein distributions and their profile changes may be associated with the biological consequences of TBI.

MALDI-MS imaging results, combined with immunohistochemical staining and other neuroimaging techniques, complement parallel metallomic studies that employ inductively coupled plasma MS, to gain anatomical and pathological understanding of focal hemorrhage and blood-brain barrier disruption as clinically-relevant consequences of impact TBI.

17. **Structure of Serum Amyloid a Suggests a Mechanism for High-Density Lipoprotein Binding and Function as a Protein Hub**
    Nicholas M. Frame & Olga Gursky

Serum Amyloid A (SAA, 12-14 kDa) is a major inducible acute-phase plasma protein conserved from sea cucumbers to humans. SAA functions in the immune response and cholesterol homeostasis via unclear mechanisms; elevated SAA causes systemic amyloidosis and contributes to cardiovascular disease. During the acute-phase response, SAA secretion into plasma increases up to 1000-fold. Most circulating SAA is bound to high-density lipoprotein (HDL, or Good Cholesterol). Although such binding is central to lipid mobilization for cell repair, the mechanism by which SAA selectively binds HDL is unclear. We combine the recently solved x-ray crystal structures of lipid-free SAA with our amino acid sequence analysis to propose such a mechanism. We identify two amphipathic alpha-helices in the N-domain of SAA (residues 1-69) which bind lipids and form a concave solvent-exposed hydrophobic surface. The curvature of this surface (radius r~4.2 nm) matches that of HDL, which explains the binding selectivity of SAA for HDL over larger lipoproteins. This curvature is maintained through a novel structural motif including GPGG residues. Our proposed mode of protein-lipid surface binding is unique to SAA and differs from any other apolipoproteins. A flexible linker starting at residue 70 of SAA connects the HDL-binding N-domain to its C-domain. The C-domain binds various polar/charged ligands including cell receptors (CD36, LOX-1) and heparan sulfate proteoglycans. The ability to bind ligands via both its domains allows SAA to bring lipoproteins and cellular receptors into contact and facilitate their functional interactions. Therefore, we propose that SAA acts as a protein hub mediating interactions among diverse proteins, lipids, and proteoglycans. Our model is supported by the observation that SAA residues 1-76, termed amyloid-A, form the major protein constituent in inflammation-linked amyloidosis. Overall, our model helps better

understand SAA's ability to perform multiple functions through its ability to bind to multiple different ligands.

18. Data-driven identification of novel molecular subclasses of COPD

Primary Authors Eric Reed1, David Bray1,Co-Authors, Stephen Lam2, Maarten van den Berge3, Gang Liu4, Xiaohui Zhang4, Yuriy Alekseyev5, Avrum Spira1,4, Marc E. Lenburg1,4, Katrina Steiling1,4

Chronic obstructive pulmonary disease (COPD) is characterized by an irreversible obstruction to airflow and affects 14.8 million people in the United States alone. Treatment options are currently limited to non-specific therapies that variably manage disease symptoms without permanently reversing airflow obstruction. This lack of effective treatments could be explained in part by our current lack of understanding the multitude of molecular mechanisms underlying the pathobiology of COPD. Our prior studies have identified COPD-associated gene expression alterations in the bronchial airway epithelium, but also significant in the expression of these genes among individuals with COPD. Here we explore this molecular heterogeneity by applying an unsupervised learning approach to sub-classify COPD patients using Affymetrix Human Gene 1.0 ST Array data. Using a linear model controlling for relevant co-variates such as age and smoking status, we first identified 3165 genes differentially expressed between individuals with (n=87) and without (n=151) COPD (FDR<0.05). We then performed hierarchical clustering coupled with dynamic tree cutting within individuals with COPD, characterizing 6 sample clusters and 8 gene clusters. A total of 7 of these gene clusters were significantly associated with expression differences across sample clusters of individuals with COPD ($p<0.05$). To validate these results we applied the same clustering approach to an independent cohort of 79 additional COPD patients. Three sample clusters identified in the discovery dataset were also identified in the validation dataset and share similar gene-cluster alterations with the training data ($p<0.05$). These findings suggest that applying data-driven approaches to identify and characterize disease subtypes in phenotypically heterogeneous diseases may ultimately improve our ability to identify distinct COPD subgroups that might benefit from targeted therapy.

19. Comprehensive Glycoproteomics of Glioblastoma Biospecimens

Chun Shao1, Joshua Klein2, Joanna Phillips3, Joseph Zaia1

Introduction: Glycosylation is one of the most common and functionally important forms of protein post-translational modifications (PTMs), which plays a central role in many biological processes and pathways, including protein folding, immune surveillance, and inflammatory reactions. The most common and widely studied forms are N-linked and O-linked glycosylation.

Aberrant glycosylation occurs during the evolution of brain cancers and neurodegenerative diseases.

The extracellular matrix (ECM) constitutes 10-20% of brain volume and provides a microenvironment for maintaining the essential functions of central nervous system. Over 80% of ECM proteins are glycosylated; however, little is known about the glycosylation pattern for brain ECM proteins. Here we present a sensitive platform to analyze N-glycoproteome and O-glycoproteome for brain ECM glycoproteins.

Method: Rat and human brain cortex histological tissue sections were cut from frozen tissue. Serial alcohol washing steps were applied to remove lipids from tissue sections. Trypsin was added to the surface of tissue section for overnight digestion. The released peptides were either enriched with hydrophilic interaction liquid chromatography (HILIC) or strong anion exchange stage tips. Half of the HILIC-enriched peptides were analyzed with C18 LC-MS/MS at Thermo-Fisher Q Exactive Plus mass spectrometer. N-glycans were released from the remaining half of the HILIC-enriched peptides with PNGase F and analyzed using an Agilent 6520 Q-TOF mass spectrometer coupled with nano-fluidic HILIC liquid chromatography. Chondroitinase ABC and heparin lyase enzymes were used to digest chondroitin sulfate (CS) and heparan sulfate (HS) chains, respectively, from peptides enriched using strong anion exchange cartridges.

Preliminary data: Brain ECM components are organized into three principal compartments: the basement membrane, the perineuronal nets and the neural interstitial matrix. Both perineuronal nets and the neural interstitial matrix comprise a dense network of hyaluronan, tenascins, link proteins, and proteoglycans. Proteoglycans are composed of a core protein to which one or multiple glycosaminoglycan (GAG) side chains attach. Chondroitin sulfate proteoglycan (CSPG) and heparan sulfate proteoglycan (HSPG) are the two major families.

We observed high levels of ECM glycoproteins from surface digestion on histological tissue sections, including CSPGs/HSPGs (brevican, versican, neurocan, CSPG4, CSPG5, and perlecan), tenascins (tenascin and tenascin R), and hyaluronan and proteoglycan link protein 1. Our data identified site specific glycosylation on ECM glycoproteins from brain. We used CAD-based tandem mass spectrometry of enriched N- and O-glycopeptides to identify peptide sequences and glycan compositions. We used the in-hous GlycoReSoft software for automated data analysis for N-glycoproteome and O-glycoproteome. Taking the versican CSPG as an example, we mapped multiple un-reported N-glycosylated, mucin type O-glycosylated, and GAG-linked sites in the core protein. We made a detailed comparison for N-glycoproteome and O-glycoproteome for human glioblastoma biospecimens and normal samples to understand the dynamic alterations of ECM glycosylation during cancer progression.

Novel aspect: This study provides a comprehensive N-glycoproteome and O-glycoproteome analysis to improve fundamental understanding of the architecture of brain ECM.

20. **Development of a culturally competent intervention targeting mental and sexual health of Asian-American young women: A Stage 1 trial of the Asian Women's Action for Resilience and Empowerment (AWARE) Intervention**
    Hyeouk Chris Hahm ;Abstract Co-Author(s): Gloria Yoonseung Lee, Christina Seowoo Lee, Sunny Sunho Lee, Mia Trentadue, Yoonsun Choi (University of Chicago)

Background: Despite their public image as "model minorities," young Asian-American women have higher rates of depression and suicide compared to their White, Black, and Hispanic counterparts. The growing incidence of substance use and HIV/AIDS in this population is alarming. To address these problems, the Asian Women's Health Initiative Project (http://bu.edu/awship) was funded by the NIMH to develop an intervention.

Objectives: (1) To describe the development of AWARE, (2) To test the efficacy of AWARE using a small pilot sample (n=9), (3) To modify the content of AWARE based on data collected from the pilot trial.

Method: Using the NIH Stage Model of intervention development as conceptual framework, we developed AWARE based on our empirical studies of the unique experiences of Asian-American women. Nine women participated in the pilot trial of AWARE, and the following data were collected: (1) ten group therapy sessions, (2) two feedback sessions, (3) post-session memos written by the therapist, and (4) three-month booster sessions. Thematic analysis was used to analyze the recordings, transcriptions, and memos.

Results: Pilot data provided evidence for the acceptability and feasibility of AWARE. Participants reported high levels of satisfaction with eight aspects: (1) culturally sensitive curriculum, (2) culturally competent therapist, (3) group psychotherapy format, (4) exploration of feelings, (5) use of technology, (6) coping skills education, (7) focus on targeting risk behaviors, and (8) session length.

Discussion: This intervention is the first and only culture- and gender-specific intervention that targets depression, suicidality, substance use, and HIV risk behaviors in Asian-American women with trauma. We utilized a comprehensive approach that incorporates various treatment modalities and culture-specific treatment content. While the randomized controlled trial of AWARE will provide more definitive evidence of its efficacy, our findings demonstrate that AWARE introduces a new empirically derived and theory-driven model for culturally adapted interventions.

21. **Technetium Pyrophosphate Cardiac Imaging in Asymptomatic Variant Transthyretin-related Cardiac Amyloidosis**

Muhammad Haq1; Co-Author: Sumeet Pawar1, Edward Miller2, John Berk3, Frederick Ruberg4

Background: Transthyretin-related cardiac amyloid (ATTR-CA) is an increasingly recognized cause of heart failure with preserved ejection fraction (HFpEF). In single center studies, technetium pyrophosphate (99mTc-PYP) cardiac imaging has noninvasively identified ATTR-CA with a quantitative heart-to-contralateral chest (H/CL) ratio threshold > 1.5. While 99mTc-PYP is well characterized in patients with overt cardiomyopathy, the utility of 99mTc-PYP in patients with variant TTR genotype (TTRm) without signs or symptoms of heart failure remains undetermined.

Objectives: To assess the utility of 99mTc-PYP cardiac imaging in patients with variant TTR genopositivity without heart failure.

Methods: Forty patients who underwent clinical examinations, echocardiography, measurement of cardiac biomarkers, and 99mTc-PYP scintigraphy (planar imaging) were subdivided into three groups: (1) patients with non-amyloid HFpEF, n = 8 (2) asymptomatic TTR mutation carriers, n = 12 and (3) TTR mutation carriers with symptoms of heart failure (ATTRm), n = 20. Cardiac retention of 99mTc-PYP was assessed using a semi-quantitative visual score (range: 0 [no uptake] to 3 [uptake greater than bone]) and H/CL ratio on planar images. Continuous and categorical variables were compared between groups.

Results: TTR mutation carriers appeared phenotypically normal compared to patients with ATTRm cardiac amyloidosis based on left ventricular ejection fraction (61 ± 8 vs 51 ± 14, p = 0.02), interventricular septal thickness (0.9 ± 0.3 vs 1.5 ± 0.3, p <0.001) and E/e' (8.1 ± 1.5 vs. 18.1 ± 8.9, p <0.001). However, abnormal 99mTc-PYP uptake was observed in the 12 asymptomatic TTR mutation carriers without heart failure as follows, grade 1 (n = 3), grade 2 (n = 3) and grade 3 (n = 4). In addition, 99mTc-PYP uptake was increased among asymptomatic carriers as compared to patients with HFpEF (H/CL ratio 1.5 ± 0.4 vs 1.2 ± 0.1, p = 0.02), but lower as compared to symptomatic ATTRm (H/CL ratio 1.5 ± 0.4 vs 1.8 ± 0.4, p = 0.02).

Conclusions: 99mTc-PYP scintigraphy demonstrated abnormal uptake by both quantitative and semi-quantitative methods among asymptomatic carriers of TTR mutations. These data suggest that abnormal 99mTc-PYP may be the first measurable manifestation of ATTR cardiac amyloidosis.

22. **Dissecting the regulatory roles of the MEF2 transcription factors in cardiac muscle**

Cody Desjardins; Francisco J. Naya

Cardiovascular disease is the leading cause of death, representing approximately 30% of documented deaths in 2012. Regardless of etiology, heart disease is associated with pathological changes in gene programs of cardiomyocytes. Thus, understanding the regulation of global gene expression in cardiomyocytes is critical to studying disease. A core gene expression regulator in the mammalian heart is the myocyte enhancer factor 2 (MEF2) transcription factors. Vertebrate MEF2 is composed of four factors that share binding activity, but *in vivo* and *in vitro* MEF2-deficiency demonstrates a distinct function for each MEF2 factor in cardiac muscle development and homeostasis. Little is understood about the gene programs regulated by each MEF2 factor, or the mechanism through which specific regulation by a single MEF2 family member occurs. Based on previous data, we propose that the MEF2 family members regulate overlapping, but distinct gene programs, and show less functional redundancy than previously reported.

We have developed shRNA-mediated reagents targeting individual *Mef2* isoforms, and are dissecting the regulatory role of the individual MEF2 factors in a primary culture model of cardiomyocytes. Initial investigations show that only the loss of *Mef2a* expression yielded a cellular phenotype, but differential expression analysis using microarrays revealed gene sets preferentially sensitive to each MEF2 factor. Further computational analysis of these preferentially regulated gene sets shows largely non-overlapping functions. Interestingly, MEF2A and –C antagonistically regulate a subset of genes, adding additional complexity to cardiac transcriptional regulation by MEF2 that has not been previously proposed. The mechanism through which MEF2 factors are recruited to the regulatory regions of sensitive genes is not well understood. These findings suggest that despite similar binding patterns, the regulatory roles of the MEF2 factors is more complicated than was appreciated, and a better understanding of the roles of individual family members is crucial to understanding cardiac homeostasis and disease.

23. **Congenital Lumbar Spinal Stenosis: Evaluation of Imaging Techniques for Greater Diagnostic Yield**

    Nishant Dwivedi1, BS, Ahmed Moussa3, MD, Nadja Kadom2, MD, Tony Tannoury3, MD, Chadi Tannoury3, MD.

Instruction: Congenital lumbar spinal stenosis (CLSS) is a developmental narrowing of the lumbar spinal canal causing chronic back pain, radiculopathy, and neurogenic claudication. It is currently unclear which radiologic method of measurement has the highest diagnostic yield for CLSS. We assessed the performance of three distinct imaging measurement techniques in order to determine the most accurate method of radiologically diagnosing CLSS. We hypothesized

that measurement of the lumbosacral Cobb angle would be the most reliable method of diagnosing CLSS.

Materials & Methods: Three measurement methods of diagnosing CLSS were evaluated in 1) 30 patients with symptomatic CLSS, 2) 30 patients with degenerative lumbar disease in the absence of CLSS, and 3) 30 patients presenting with back pain in the absence of imaging pathology. Method 1: Ratio of the anterior-posterior (AP) vertebral body (VB) diameter and spinal canal AP diameter at L3 on radiographs and MRI; Method 2: Ratio of VB and spinal canal cross-sectional area at L3 on MRI; Method 3: Measurement of the L2-S1 lumbosacral angle on radiographs. Statistics: Inter-rater reliability and regression (Stata 13.1, Texas, USA).

Results: All measurement methods showed almost perfect reproducibility (intra-class r>0.81). CLSS displayed a greater association with male gender (p=0.023) and younger age (p=0.007). BMI was highest in patients with CLSS and showed a trend (p=0.057). The measurement methods that best correlated with a diagnosis were Method 2 (p=0.012) and Method 3 (p=0.009).

Conclusion: 1-The best radiologic techniques for diagnosing CLSS are the measurement of the ratio of the vertebral body to the spinal canal cross-sectional area on MRI and of the lumbosacral angle between L2-S1 using the Cobb method on radiographs.

2-The ability to reliably diagnosis CLSS through imaging prior to pursuing surgical interventions may greatly inform clinical decision-making and provide essential information for prognostic counseling of patients.

24. Disposable Cartridge Platform for Rapid Multiplex Detection of Viral Hemorrhagic Pathogens from Plasma and Whole Blood

Steven M. Scherr1*, David Freedman2, Helen Fawcett1, Selim Unlu3,4,5, John Connor6

Real-time, sensitive detection of individual viruses at the point-of-care is necessary for the control and treatment of viral hemorrhagic fevers such as Ebola, Lassa, and Marburg. A successful diagnostic test at the point-of-care must be rapid, sensitive, and inexpensive, while needing minimal sample preparation or user expertise. There are currently no multiplex techniques for diagnosing Ebola in the field that meet these requirements. We have developed a hybrid polymer-paper microfluidic cartridge with an integrated optical Interference Reflectance Imaging Sensor (SP-IRIS) to perform rapid detection of individual viruses directly in human plasma or whole blood. By incorporating paper based fluid handling and on-chip plasma separation we were able to greatly reduce the need for external equipment and sample preparation. Using a fully automated nanoVision instrument we have shown detection of

recombinant vesicular stomatitis virus psuedotypes of Ebola virus (ZEBOV), Marburg virus (MARV), and Lassa virus (LASV), as well as Ebola Virus-like-particles in less than 20 minutes. This platform is adaptable for the detection of many different viruses and promises to simplify and reduce the cost of rapid diagnostics and improve our ability to control and prevent disease.

25. **Determine optimal culture and dosage conditions for Rothia bacteria degrading gluten in the TIM-1 human digestion model**

    Chin-Hua Yang, Ghassan Darwish, Na Tian, Guoxian Wei, Eva J. Helmerhorst

Introduction: Celiac disease is a T-cell mediated-inflammatory disorder of the small intestine precipitated by gluten ingestion. Gluten can be effectively degraded by Rothia aeria, a natural resident oral microbe. It is hypothesized that Rothia bacteria can degrade and detoxify gluten in vivo and can be developed as a first probiotic for celiac disease. Aims. To select the optimal culture conditions for R. aeria enzyme expression in vitro and determine the required R. aeria to gluten ratio to achieve digestion within 2h, the residence time of foods in the stomach/upper intestines.

Methods: R. aeria culture variables evaluated were dilutions of Brain Heart Infusion (BHI; 4%, 20% and 100%), temperature (28oC and 37oC), pH (4.0 and 7.0), carbon sources (glucose, succinate, glycerol, or casein) added to M9 minimal salts, and cultivation time (16-72h). Enzyme activities in suspensions normalized for optical density (OD) were measured with a paranitroanilide-derivatized enzyme substrate. Gliadin degradation was investigated with a fixed gliadin concentration (250 µg/ml) and various R. aeria cell densities (OD620 1.0, 0.5, 0.25), and was monitored by SDS-PAGE. Results. Enzyme activity was minimally affected by BHI broth strength or cultivation times. Cells grown at 37oC showed on average a higher enzyme activity than cells grown at 28oC. No bacterial growth was observed at pH 4.0, or in M9 broth +2% glucose, succinate, or glycerol. Enzyme activities in M9+2% casein were lower than in BHI. As expected, gliadin degradation rates decreased with decreasing R. aeria cell density.

Conclusions: Full strength BHI broth and 72h cultivation at 37°C were ultimately chosen as the cultivation condition to obtain high R. aeria cell numbers. Based on the dosage experiments a 1:1 ratio of R. aeria OD620 1.0mg gluten was chosen for future studies in an in vitro human digestion model. Supported by NIH/NIAID grants AI087803 and AI101067.

26. **Modeling Sickle Cell Anemia Using Induced Pluripotent Stem Cells**

    Seonmi Park1, Andreia Gianotti-Sommer1, David H. K. Chui1, Maria Stella Figueiredo2, Abdulrahman Alsultan3. Amein Al-Ali4, Martin H. Steinberg1, George Murphy1, Gustavo Mostoslavsky1

Background: Sickle cell anemia (HBB rs334glu6val) had independent origins in Africa, the Middle East and India and spread throughout parts of the world by wars, slave trading and population migrations. The genetic background on which the HbS mutation occurred, or the β-globin gene haplotype, is associated with differences in the phenotype of this disease and the ability to synthesize fetal hemoglobin (HbF). HbF is the main modifier of the disease phenotype.by its inhibition of HbS polymerization. Objective and Hypothesis: By establishing a library of induced pluripotent stem cells (iPSC) from patients with sickle cell anemia of diverse HBB haplotypes and HbF phenotypes, genetic studies of globin gene expression during the erythroid differentiation of iPSC would increase our ability to model variation in HbF expression.

Methods: Samples from African Americans with diverse HBB haplotypes, predominantly homozygotes and compound heterozygotes for the Benin and Bantu haplotypes, Saudi Arabians with the Arab-Indian haplotype and the Saudi Benin haplotype and Brazilians who are predominantly homozygotes for the Bantu haplotype typically associated with low HbF were generated using the STEMCCA platform. Results: We performed RNA sequencing using Digital Gene Expression (DGE) analysis comparing either CD34-peripheral blood-derived erythroid progenitors to iPSC-derived erythroid progenitors to identify key pathways involved in the specification of the erythrocyte lineage with a specific globin expression profile. DGE comparison of normal vs. sickle cell lines identified key differences between the specific haplotypes that may help understand the inherent differences in HbF levels present in these individuals. We developed a CRISPR-based gene editing platform and corrected the sickle mutation in iPSC preparing the next generation tools for personalized therapy.

Conclusions: The ability to directly differentiate iPSCs of patients with sickle cell anemia can serve as a drug screening platform for HbF inducers and perhaps therapeutically as a definitive cellular-based therapy.

27. **Single Cell RNA Sequencing Reveals Smoking-Associated Alterations in Bronchial Epithelial Subpopulations**

    Grant E. Duclos1,2, Yves M. Dumas1, Patrick Autissier3, Robert Terrano1, Gang Liu1, Marc E Lenburg1, Avrum Spira1, Joshua D. Campbell1, Jennifer Beane1

Rationale: Bronchial epithelial gene expression reflects the physiologic response to cigarette smoke exposure. In this study, we use single cell RNA-seq to profile the transcriptomes of individual bronchial epithelial cells obtained from current and never smokers. The single cell resolution will allow us to detect smoking-associated alterations within specific epithelial cell types, shifts in cell type abundance, and discover novel cell types affected by tobacco exposure.

Methods: We obtained bronchial brushings from current smokers (n=6) and never smokers (n=6) and isolated single epithelial cells by FACS. The CEL-Seq RNA library preparation protocol was used to simultaneously sequence the transcriptomes of 1,008 cells (n=84/donor). Principal component analysis was used to identify transcriptomically distinct cellular subsets. Negative binomial generalized linear models were used to identify genes whose expression was significantly associated with smoking status (FDR q < 0.05) within specific subsets. Sets of differentially expressed (DE) genes were functionally annotated using MSigDB and intersected with our previously published smoking-associated bronchial gene expression signature.

Results: The three distinct cellular subpopulations were enriched with cells expressing KRT5, MUC5AC, or FOXJ1, indicating the presence of basal, secretory, and multiciliated airway epithelial cells, respectively. Decreased numbers of basal cells and increased numbers of secretory cells were observed in tissue obtained from smokers. Previously identified smoking-associated DE genes were localized to distinct cellular populations. Additionally, genes involved in the response to interferon gamma signaling were specifically up-regulated in smoker secretory cells, whereas genes involved in the response to xenobiotic stress were up-regulated across all smoker cells.

Conclusion: The bronchial gene expression response to smoking is an ensemble of responses from multiple cell types that were not previously captured by profiling bulk cell populations. These results may allow us to better interpret the molecular consequences of smoking on the bronchial epithelium and elucidate smoking-related contributions to disease pathogenesis.

28. **Detection of Tumor-specific Mutations in Circulating, Cell-free DNA: Potential for a Biomarker in Esophageal Adenocarcinoma**
    Matthew Egyud1, Jennifer Jackson1, Emiko Yamada1, Anders Stahlberg1,2, Virginia Litle1, and Tony Godfrey1*

Background: Esophageal adenocarcinoma (EAC) has increased in incidence parallel with gastroesophageal reflux disease and 5-year survival is poor. Management of patients with EAC is complicated by late diagnosis and poor response to therapy. Recent studies have shown that tumor-specific DNA can be detected circulating in plasma and this raises the possibility of "liquid biopsies" using mutated tumor DNA as a potential diagnostic and prognostic biomarker. We have developed a novel approach to introduce molecular barcodes into sequencing libraries with DNA inputs as low as 5ng. Barcodes enable differentiation of true mutants from background noise introduced by Taq polymerase errors and permits detection of variant alleles with frequencies below 0.1%. The barcodes are protected from mis-priming using a hairpin structure which permits a high degree of multiplexing, allowing us to assay multiple mutations

from one plasma sample. We are using this technology to test the utility of liquid biopsy as a biomarker for esophageal adenocarcinoma diagnosis and disease monitoring.

Methods: Blood samples were obtained at a single time point from patients with various stages of EAC and longitudinal blood samples were also collected from patients undergoing neoadjuvant therapy followed by surgery. Tumor samples were obtained from biopsy or resection specimens. DNA was sequenced using a targeted EAC panel to identify mutations in the tumor. Assays were designed to identify these mutations in plasma, and hairpin barcodes were attached. Sequencing libraries were generated from circulating DNA, sequenced and analyzed using the barcodes to reduce background noise.

Results: Mutations were identified in tumor samples from 32 patients. Of 18 analyzed to date, the same mutations have been identified in 7 plasma DNA samples. All mutant alleles were present at <1% frequency and two patients demonstrated multiple mutant alleles in plasma DNA. Data on the full cohort and on longitudinal samples to monitor therapy response will be presented.

Discussion: Tumor DNA can be detected in the plasma of patients with EAC using ultra-sensitive sequencing. Possible applications include prognostication in early stage patients and rapid monitoring of therapeutic response and recurrence. Further work is to evaluate this is ongoing.

29. **Dimethyl Fumarate Ameliorates Pulmonary Hypertension in vivo and Prevents Fibrosis via βTRCP Mediated Degradation of β-catenin and TAZ**
    Agnieszka Grzegorzewska1, Rong Han1, Francesca Seta2, Lukasz Stawski1, Carol Feghali-Bostwick4, Jeffrey Browning3, Maria Trojanowska1.

Introduction: Pulmonary arterial hypertension (PAH) is a serious, progressive and fatal complication of systemic sclerosis (SSc). Oxidative stress and chronic inflammation have been shown to play important roles in pathogenesis of PAH. Dimethyl Fumarate (DMF) (Tecfidera®) is an anti-oxidative and anti-inflammatory agent approved by the FDA for treatment of multiple sclerosis. In this study we test DMF as a potential drug to treat PAH.

Methods: DMF was administered daily via intraperitoneal injections in a chronic hypoxia mouse model of PAH in preventive and therapeutic modes as well as preventively in a bleomycin lung fibrosis model. In vitro studies were performed on human primary arterial endothelial cells and primary human lung fibroblasts from SSc patients and healthy controls. Endothelial cells were exposed to hypoxic conditions or lipopolisaccharade (LPS) in combination with DMF or vehicle treatment. Pulmonary fibroblasts were treated with transforming growth factor beta (TGFβ) and DMF or vehicle.

Results: DMF prevented and reversed hemodynamic changes and right ventricular hypertrophy as well as reduced inflammation, oxidative stress and vascular muscularization in a mouse PAH model. DMF improved the function of cultured endothelial cells by normalizing hypoxia induced gene expression of pro-inflammatory cytokines and growth factors via inhibition of NFκB, STAT3 and JNK signaling. DMF also suppressed TGFβ dependent pro-fibrotic gene expression in cultured human lung fibroblasts. Studies of endothelial cells and fibroblasts indicated that Nuclear factor (erythroid-derived 2)-like 2 (NRF2) -mediated anti-oxidative pathway is dispensable for the anti-inflammatory and anti-fibrogenic properties of DMF. In fibroblasts, DMF had no significant effect on canonical TGFβ signaling, but instead led to ubiquitin ligase-βTRCP mediated degradation of the pro-fibrogenic transcription factors Sp1, TAZ and β-catenin. In vivo validation of anti-fibrotic DMF properties in a bleomycin mouse model indicated that the drug prevented development of lung fibrosis in a manner correlated with a reduction in active β-catenin levels by immunostaining.

Conclusions: In conclusion, DMF has anti-oxidative, anti-inflammatory and anti-fibrotic potential both in vitro and in vivo. Given the safety profile of Tecfidera® and its pleiotropic mechanism of action, it may provide an effective treatment for SSc-PAH.

30. PDGFRβ is a novel marker of stromal activation in oral squamous cell carcinomas

Vinay K. Kartha1, 2, Lukasz Stawski3, Rong Han3, Paul Haines3, George Gallagher4, Vikki Noonan4, Maria Kukuruzinska5, Stefano Monti2&, Maria Trojanowska3&

Carcinoma associated fibroblasts (CAFs) form the main constituents of tumor stroma and play an important role in tumor growth and invasion. The presence of CAFs is a strong predictor of poor prognosis of head and neck squamous cell carcinoma. Despite significant progress in determining the role of CAFs in tumor progression, the mechanisms contributing to their activation remain poorly characterized, in part due to fibroblast heterogeneity and the scarcity of reliable fibroblast surface markers. To search for such markers in oral squamous cell carcinoma (OSCC), we applied a novel approach that uses RNA-sequencing data derived from the cancer genome atlas (TCGA). Specifically, our strategy allowed for an unbiased identification of genes whose expression was closely associated with a set of bona fide stroma-specific transcripts, namely the interstitial collagens COL1A1, COL1A2, and COL3A1. Among the top hits were genes involved in cellular matrix remodeling and tumor invasion and migration, including platelet-derived growth factor receptor beta (PDGFRβ), which was found to be the highest-ranking receptor protein genome-wide. Similar analyses performed on ten additional TCGA cancer datasets revealed that other tumor types shared CAF markers with OSCC, including PDGFRβ□□which was found to significantly correlate with the reference collagen expression in ten of the 11 cancer types tested. Subsequent immunostaining of OSCC specimens demonstrated that PDGFRβ was abundantly expressed in stromal fibroblasts of all

tested cases (12/12), while it was absent in tumor cells, with greater specificity than other known markers such as alpha smooth muscle actin or podoplanin (3/11). Overall, this study identified PDGFRβ as a novel marker of stromal activation in OSCC, and further characterized a list of promising candidate CAF markers that may be relevant to other carcinomas. Our novel approach provides for a fast and accurate method to identify CAF markers without the need for large-scale immunostaining experiments.

31. **Altered RNA editing in 3' UTR perturbs microRNA-mediated regulation of oncogenes and tumor-suppressors**
    Liye Zhang1,*, Chih-Sheng Yang2, Xaralabos Varelas2, Stefano Monti1,*

RNA editing is a molecular event that alters specific nucleotides in RNA post-transcriptionally. RNA editing has the potential to impact a variety of cellular processes and is implicated in diseases such as cancer. Yet, the precise mechanisms by which RNA editing controls cellular processes are poorly understood. Here, we characterize sequences altered by RNA editing in patient samples from lymphoma, neuroblastoma and head and neck cancers. We show that A-to-I RNA editing sites are highly conserved across samples of the same tissue type and that most editing sites identified in tumors are also detectable in normal tissues. Next, we identify the significant changes in editing levels of known sites between tumor and paired "normal" tissues across 14 cancer types (627 pairs) from The Cancer Genome Atlas project and show that the complexity of RNA editing regulation cannot be captured by the activity of ADAR family genes alone. Our pan-cancer analysis confirms previous results on individual tumor types and suggests that changes of RNA editing levels in coding and 3'UTR regions could be a general mechanism to promote tumor growth by perturbing microRNA meditated regulation. We also propose a model explaining how altered RNA editing levels affect microRNA-mediated post-transcriptional regulation of oncogenes and tumor-suppressors.

32. **Is negative co-testing in HIV+ women associated with a lower three-year risk of cervical pre-cancers?**
    Rachel Alade, M.S., Elizabeth A. Stier, MD

Objective: HIV+ women are more likely to have persistent cervical HPV infections, cervical neoplasia, and cervical cancer compared with HIV- women. Cervical cancer screening guidelines for HIV+ women include annual cervical cytology collection, but the role of HPV co-testing is unclear. We assessed whether HIV+ women, ≥30 years with normal cytology/negative HPV (-/-) co-testing could safely lengthen the screening interval.

Methods: We conducted a retrospective chart review of HIV+ women aged ≥30 with normal, index cervical cytology between 11/2008-12/2010 and at least 1 subsequent cytology at Boston

Medical Center. Based on the HPV co-testing result associated with the baseline cytology, we compared the incidence of subsequent CIN-2+ development through 12/2014.

Results: 48 of the 326 (14.7%) HIV+ women with normal index cytology tested HPV+ at baseline. HIV+/HPV+ women were more likely to be subsequently diagnosed with CIN-2+ (4/48 (8.3%)) when compared with HIV+/HPV- women (9/278 (3.2%) (OR: 2.459; 95%CI: 0.707-8.554)). Mean interval for diagnosis of CIN-2+ in HIV+/HPV+ women compared with HIV+/HPV- women was 338 days (121-538) vs. 1117 days (503-2036) respectively ($p<0.025$).

Conclusions: This clinical data supports the findings of the WIHS cohort, research study - HIV+ women undergoing cervical cancer screening, who are HPV- with normal cytology, have a low risk of being diagnosed with CIN-2+ within the next 3 years. Thus, the cervical cancer screening interval for HIV+ women with -/- co-testing may be safely increased from 1 to 3 years. However, HIV+ women with HPV+ testing, even with normal cytology, need to be followed closely as these women have a significant future risk of CIN-2+ diagnosis.

33. Estimating Default Mode Network Connectivity with Cardiorespiratory Fitness
Corey Kronman

Human studies and animal models have linked changes in the Default Mode Network (DMN) to Alzheimer's Disease (AD). In particular, AD is accompanied by weaker functional connectivity (FC), diminished effective connectivity (EC), and greater atrophy within the hippocampus and the posterior cingulate cortex. Previous studies have demonstrated that aerobic exercise leads to greater cardiorespiratory fitness, and DMN FC in healthy adults. The goal of this study is to investigate how cardiorespiratory fitness may be used to predict DMN EC in sedentary young adults. We hypothesize that individuals exhibiting greater cardiorespiratory fitness will display greater effective connectivity within the DMN. To investigate our hypothesis, we analyzed data from from 25 sedentary young adults. Data included a resting state fMRI procedure and a physical fitness test, each taken from part of a larger ongoing clinical trial in the BPN Lab at BU. We utilized group ICA to define the regions of the DMN and CGCA to determine EC between these regions. ICA indicated 9 significant regions in the DMN, consistent with previous work. This results in 72 possible pairs of DMN regions for CGCA. We created linear regression models to analyze the effect of cardiorespiratory fitness on EC between DMN regions and found 11 linear models which exhibited a significant ($p > 0.05$) relationship. Eight of eleven models involved the left or right hippocampus, showing that greater cardiorespiratory fitness levels are correlated with greater EC with the hippocampus in the DMN. These results provide proof of concept that greater cardiorespiratory fitness is correlated with stronger DMN EC, particularly involving the hippocampus. This adds to the literature suggesting extended aerobic exercise, which has been shown to increase physical fitness, may help to diminish the threat of

neurological pathologies associated with AD. Further investigation is required to explore this use of aerobic exercise intervention.

34. Predicting hospital re-admissions for surgical patients

Taiyao Wang, Tingting Xu, Theodora Brisimi, George Kasotakis, and Ioannis Ch. Paschalidis

Changes in federal regulations for the health care industry, as well as, payment penalties imposed to hospitals based on quality of care metrics, provide strong incentives to improve the quality and value of the services offered to patients. Specifically, the Hospital Readmission Reduction Program (HRRP) penalizes hospitals with 30-day readmission rates higher than the national average by decreasing their reimbursements from Medicare. This motivates our research which aims to predict re-admissions for patients who have been hospitalized to undergo a general surgery procedure. Our data set consists of pre-operative, intra-operative, and post-operative outcomes that were recorded using the standard National Surgical Quality Improvement Project protocol (ACS NSQIP) for patients who had a general surgery procedure at the Boston Medical Center (BMC) between 2010 and 2013. We aim to predict 30-day re-admissions and identify factors related to the re-admissions by exploring a variety of supervised classification methods, such as Support Vector Machines (SVM), Sparse Linear Support Vector Machines (SLSVM), Random Forests, and L1/L2-regularized Logistic Regression. Experimental results using data from BMC demonstrate good prediction accuracy as well as meaningful vital factors, which allow us to provide an interpretation of the outcomes generated by the lassification models.

35. Tai Chi for Posttraumatic Stress Disorder (PTSD): Satisfaction and Qualitative Findings

Craig Polizzi1,2; Barbara L. Niles, Ph.D.1,2,3, Deanna L. Mori, Ph.D.2,3, Anica Pless aiser, Ph.D.1,2,3 and Chenchen Wang, M.D., MSc.4

Introduction: Posttraumatic Stress Disorder (PTSD) affects up to 20% of Veterans and is associated with numerous psychosocial and physical ailments. Previous research has shown that Tai Chi, a traditional Chinese mind-body exercise, can improve physical and mental health in populations with chronic conditions. The goal of this study was to evaluate the feasibility and satisfaction of a 4-session preliminary Tai Chi program for Veterans with PTSD symptoms.

Methods: Seventeen Veterans participated in this Tai Chi program. A mixed methods approach was used to analyze the data. Participants used Likert-scale self-report questionnaires to evaluate their satisfaction with the Tai Chi program. Also, a focus group and individual

interviews were conducted after the final session. These qualitative data were transcribed and analyzed by a committee of reviewers.

Results: General satisfaction with the Tai Chi program was very high, as 94% of Veterans reported that they were very or mostly satisfied with the program, with the amount of help they received, and that the quality of the program was excellent or good. 69% endorsed that Tai Chi helped them to deal more effectively with their problems, an unanticipated finding given the brevity of the program. 100% endorsed that they would participate in future Tai Chi programs again. The qualitative analysis revealed that participants attributed numerous benefits to Tai Chi including calming the mind, relaxing the body, low impact, feelings of accomplishment, hope, and optimism, and motivation to do more exercise. Tai Chi was also perceived as a program that can be done by any individual, despite age or physical limitations.

Conclusions: Satisfaction ratings and qualitative findings indicate that Tai Chi is a well-received, feasible and acceptable intervention for Veterans with PTSD. Findings from this study suggest that Tai Chi is deserving of larger-scale clinical trials for Veterans with post-deployment distress in the future.

36. Targeting Wnt/□-catenin/CBP Axis in Oral Cancer

*Khalid Alamoud1, Khikmet Sadykov1, Manish Bais1, Vinay Kartha2, Stefano Monti2, Anna Belkina3, Jennifer Cappione3, and Maria Kukuruzinska1

Introduction: Oral squamous cell carcinoma (OSCC) represents the majority of head and neck cancers and is associated with high mortality and few therapeutic options available. Evidence suggests that aggressive cancers arise from tumor propagating cells (TPCs) that exhibit the properties of stem cells and may drive tumor development, recurrence and resistance to therapy. The Wnt/□-catenin/CBP signaling cascade and protein N-glycosylation play important roles in OSCC and stem cell phenotypes and function in a positive feedback loop. Our studies indicate that aberrant activation of □-catenin and N-glycosylation promotes OSCC and the TPC state. We hypothesize that inhibition of □-catenin/CBP axis will inhibit OSCC growth and metastasis.

Methods: Using 16-color flow cytometry we carried out phenotypic characterization of oral TPCs from OSCC cell lines and fresh human tumor specimens. The roles of □-catenin/CBP signaling were determined by pharmacological knockdown and examination of □-catenin, E-cadherin, N-glycosylation-regulating gene, DPAGT1, and vimentin levels and localization in vitro and analyses of orthotopic tumors in nude mice.

Results: FACS sorting of metastatic OSCC HSC3 and non-metastatic CAL27 cells using lectins PHA+ (high N-glycosylation) and ConA+ (low N-glycosylation), revealed a much greater fraction

of PHA+ HSC3 cells than CAL27 cells that aligned with increased nuclear □-catenin, suggesting N-glycosylation/□-catenin were associated with OSCC metastatic phenotypes. Flow cytometry analyses of fresh OSCC human tumor specimens identified a subpopulation of PHA+ cells co-expressing CD44+ or CD29+ primitive cell surface markers. Inhibition of □-catenin-CBP interaction with ICG-001 reduced DPAGT1/N-glycosylation, enhanced E-cadherin adhesion and led to growth arrest. Further, treatment of human HSC3-cell line-derived orthotopic tongue tumors with ICG-001 in nude mice inhibited tumor growth and metastases, while reducing DPAGT1 and vimentin expression and enhancing E-cadherin adhesion.

Conclusion: Results suggest that targeting □-catenin/CBP interaction may represent a novel therapeutic for the treatment of OSCC in humans.

37. CK2 is necessary for Wnt-dependent stabilization of β-catenin

Melissa Ming Jie Chua[1], Isabel M. Dominguez[1]

Introduction: CK2 is a highly conserved serine/threonine kinase family. CK2 has been found to participate in a large variety of signaling pathways, with a diverse number of substrates. In the Dominguez laboratory, CK2 has previously been found to regulate Wnt signaling. Wnt signaling is important for early embryonic development. Wnt signaling upregulates β-catenin, the transcriptional co-factor in the Wnt signaling pathway.

When aberrantly overexpressed, CK2 can serve as an oncogene, and thus has been implicated in cancer. Additionally, β-catenin stabilization has been found to occur in human tumors. In CK2 transgenic mice, β-catenin is overexpressed in mammary tumors and thus promoting tumorigenesis (Seldin, 2005). However, the mechanism by which CK2 regulates Wnt signaling is unknown.

Methods: Cell culture and Wnt signaling

C57MG and L cells were obtained from the lab and cultured in DMEM cell culture. L cells were used to culture Wnt-3a and control medium. The C57MG cells were treated with DMSO (vehicle control) and either 5.5mM or 16.6mM Qunalizatin (CK2 inhibitor). The cells were incubated with Wnt-3a and collected at 0, 0.5, 1.5, 2.5, 3.5, and 4.5h time points. The samples were assayed for protein concentration using the Pierce BCA assay.

Western blot

Samples from lysed cells as above in 1 were loaded onto an SDS-PAGE gel and run for ~90min, with a protein ladder. The gel was transferred to a membrane and analyzed for CK2α and β-

catenin protein levels using antibodies against them. The gels were analyzed using Multigauge software.

Results: Inhibition of CK2 led to a dose-dependent decrease of β-catenin protein levels in the presence of Wnt stimulation.

Conclusions: These results indicate that CK2 is necessary for Wnt-dependent stabilization of β-catenin. Stabilization of β-catenin has been implicated in many cancers. Thus, CK2 presents as a potential therapeutic target in tumor control.

38. Request Not to Publish

39. Quantitative T2 analysis of human cardiac amyloidosis samples

Ning Hua[1] ; Jennifer Ellis Ward[2], Varuna Shibad[2], Grace Yee[1], Lawreen H. Connors[2], Hernan Jara[3], David Seldin[2], and James A. Hamilton[2]

Immunoglobulin Light Chain Cardiac Amyloidosis (ALCA) is caused by extracellular deposition of abnormally folded protein (amyloid) which damages the heart. ALCA is linked to poor prognosis with a<30% survival rate within 2 years of clinical manifestation. An accurate assessment of amyloid deposition at different stages would complement current diagnostic methods, such as echocardiography and endomyocardial biopsy, and would provide a non-invasive means to monitor disease progression and therapeutic responses. Here we explore the potential of using quantitative T2 relaxation MRI to assess the degrees of ALCA in ex-vivo tissues.

Methods: Human myocardial specimens from 7 ALCA patients and 2 controls were studied. Frozen specimens stored at -20°C were thawed to room temperature, and imaged at 25°C using a Bruker 11.7T Avance instrument and a 20 mm birdcage coil. A Multi Slice Multi Echo sequence was applied: FOV=15mm^2, matrix size=64x64, slice thickness=1.25mm, slice number= 4-13, TR=4000ms, echo spacing=6.4ms, echo=32, NEX=32. T2 values were calculated using non-linear least squares fitting. The T2 distribution pattern was assessed by the mathematically calculated skewness (0=symmetric). Specimens were classified into 3 categories based on Congo-Red staining: 0, controls; 1+, focal amyloid deposit; 2+, diffused interstitial amyloid deposit. Data are presented as mean ±SD. Statistical significance is considered as p >0.05.

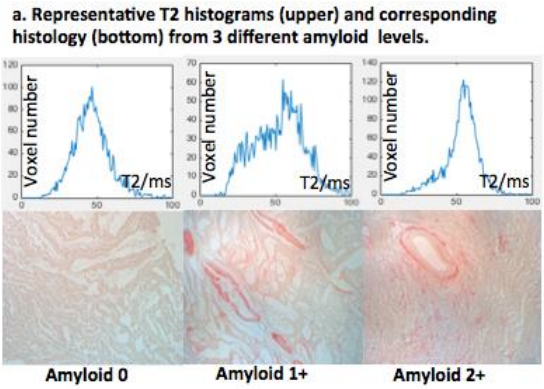

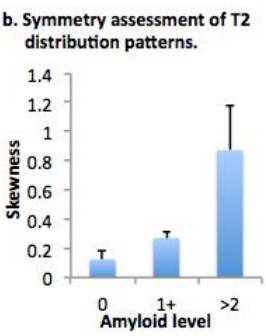

Results: Mean T2 values were comparable between ALCA and control groups (46.1±10.1ms vs. 48.3±3.5ms; p=0.77), but the distribution pattern differed. Non-amyloid samples showed a more symmetric distribution of T2 (skewness=0.12±0.05, Figure 1); whereas ALCA samples showed asymmetric pattern. Skewness increased with the amount of amyloid present: ALCA level 1+ =0.27±0.04, ALCA level 2+ =0.87±0.31.

Conclusions: The asymmetry of T2 distribution differs in each of the three stages examined, and increases as ALCA progresses. The MRI sequences can be applied in vivo, and could provide a new means to diagnose and monitor the disease.

40. **Implementation of "Oncogrid" a mobile telemedicine model for early diagnosis of oral cancer in resource restricted settings**
    Poornima Kadagad; Abstract Co-Author: Radhika Chigurupati

Background: Over 60% of the oral cancer cases in Low and Middle-Income Countries (LMIC) are diagnosed at an advanced stage. The reasons for delay in diagnosis are affected by numerous factors including the provider, the patient and the healthcare infrastructure. Early diagnosis of oral cancer requires an effective screening method. The most cost-effective method is available is visual inspection of the oral cavity by trained health workers.

Aim: To implement “Oncogrid” a mobile telemedicine model for early diagnosis of oral cancer in resource limited settings.

Hypothesis: Oncogrid mobile telemedicine model facilitates early diagnosis of oral cancer by frontline health workers in resource limited settings

Methods: The Oncogrid mobile health model has two interfaces, the front end which is a mobile phone application and a back end which is a web-based application. A custom application on a mobile phone has been programmed to assess behavioral risk factors and clinical characteristics to diagnose premalignant and malignant oral lesions, and a web application which allows a remote specialist to retrieve the patient data to make a diagnosis and recommendations for biopsy or follow up by a specialist.

Results: This project was implemented in four dental schools in India. Sixteen hundred participants were screened and 900 remote diagnosis were completed.

Conclusions: Our proposed model has shown that it has a potential to improve oral cancer screening and early diagnosis and provide pathway for early referral in rural and low resource settings. Challenges we faced in order to complete the loop of remote diagnosis and referral were mostly related to image quality and technology/internet. As a next step, we propose to refine and improve the mobile application for risk assessment and diagnosis of oral cancer using an intelligent image analysis algorithm to make the recommendations at the point of care.

41. Identification of activated stromal cells in breast cancer

Carl A. Ceraolo, BS; Ana de la Cueva, PhD, Kathrin H. Kirsch, PhD, Matthew D. Layne, PhD

Epithelial-derived cancers such as breast cancer consist of transformed epithelial cells surrounded by a stroma containing numerous cell types. It is unknown how stromal cells expressing both smooth muscle actin (SMA) and type I collagen (Col) communicate with transformed epithelial cells to promote tumor growth and metastasis. Understanding the kinetics of stromal activation and characterizing both the cell types involved in cancer stroma and their secreted proteins may lead to future therapies to stop breast cancer progression. We hypothesize that changes in breast cancer stroma, particularly an increase in SMA expression in stromal fibroblasts, drive cancer progression. Our objective is to develop a novel in vivo mouse model to track and isolate activated cells in breast cancer stroma.

To identify changes in breast cancer stroma we crossed mice expressing the Her2/neu receptor, which occurs in 20-30% of human breast cancers, with transgenic mice harboring SMA (SMA-GFPChry) and collagen (Col-GFPTpz) driving red and green variants of green fluorescent protein (GFP) respectively. Initial experiments characterized expression of these reporters at baseline in vivo and how they responded to stimuli in vitro. A new method to detect fluorescent reporter activity was developed, and at 36 weeks tumor and mammary gland tissue were isolated.

Sections of tumors and the surrounding stroma were analyzed. Three distinct cell populations were observed: those expressing SMA, those expressing Col, and those expressing both. In tumor sections Col+ cells were abundant and dispersed on the tumor margin. Few double SMA+ and Col+ were detected.

In summary, we developed a new model to detect changes in breast cancer stroma as well as a procedure for preserving fluorescence in mouse tissue for analysis. Ongoing work will characterize stromal cells by flow cytometry and expression profiling and develop strategies to target stroma-derived proteins to treat breast cancer.

42. Mining CK2 in Cancer

Ortega C, Seidner Y and Dominguez I

CK2 is a serine-threonine kinase involved in cell growth, cell proliferation and cell apoptosis, that is oncogenic when overexpressed in mouse tissues. CK2□ protein is elevated in human tumors, however, we have little information on CK2□' and CK2□ proteins, and scarce information on CK2 gene transcript expression. Therefore, we had tow objectives: 1) to assess the expression of CK2 transcripts (CK2□, CK2□, CK2□' and CK2□ pseudogene (CK2□P)) in primary tumor tissues in the six most prevalent cancers in the USA using Oncomine analysis, and 2) to

determine whether CK2 transcript expression correlates with overall survival in three of these cancers using Kaplan-Meier Plotter analysis. We analyzed the results for their p-value and fold change in the different cancer types.

We found CK2 overexpressed in all six cancers studied. For CK2 and CK2' results differ depending of type or subtype of cancer. CK2 was overexpressed except in lung cancer where it was either over- or under-expressed. CK2 transcripts were upregulated in both ductal and lobular invasive breast carcinoma. CK2' was upregulated in lung, colorectal, and prostate cancers and is downregulated in breast, ovarian, and pancreatic cancers. CK2P was upregulated in lung, breast, and colorectal cancers. In general, higher levels of CK2 gene expression led to lower survival amongst patients with lung, breast, and ovarian cancer. However, in lung adenocarcinoma, higher levels of CK2α' and CK2αP correlated with higher survival rates.

In conclusion, we show that CK2 gene transcript expression and its effect on patient survival varies with tumor type. These data provides additional evidence for CK2 as a biomarker for cancer studies and as a target for cancer therapy. The potential CK2 expression deregulation has on cancer patient diagnosis, treatment and survival needs to be further evaluated.

43. The TCA Cycle Transferase DLST Is Important For MYC-mediated Leukemogenesis

NM Anderson1, D Li1, HL Peng2,3, FJF Laroche1, MR Mansour2, E Gjini2, M Aioub1, DJ Helman2, JE Roderick4, T Cheng1, I Harrold1, Y Samaha1, L Meng1, A Amsterdam5, DS Neuberg6, TT Denton7, T Sanda8, MA Kelliher4, A Singh1, AT Look2, H Feng1*

Despite the pivotal role of MYC in the pathogenesis of T-cell acute lymphoblastic leukemia (T-ALL) and many other cancers, the mechanisms underlying MYC-mediated tumorigenesis remain inadequately understood. Here we utilized a well-characterized zebrafish model of Myc-induced T-ALL for genetic studies to identify novel genes contributing to disease onset. We found that heterozygous inactivation of a tricarboxylic acid (TCA) cycle enzyme, dihydrolipoamide S-succinyltransferase (Dlst), significantly delayed tumor onset in zebrafish without detectable effects on fish development. DLST is the E2 transferase of the -ketoglutarate dehydrogenase complex (KGDHC), which converts -ketoglutarate (-KG) to succinyl-CoA in the TCA cycle. RNAi knockdown of DLST led to decreased cell viability and induction of apoptosis in human T-ALL cell lines. Polar metabolomics profiling revealed that the TCA cycle was disrupted by DLST knockdown in human T-ALL cells, as demonstrated by an accumulation of -KG and a decrease of succinyl-CoA. Addition of succinate, the downstream TCA cycle intermediate, to human T-ALL cells was sufficient to rescue defects in cell viability caused by DLST inactivation. Together, our studies uncovered an important role for DLST in

MYC-mediated leukemogenesis and demonstrated the metabolic dependence of T-lymphoblasts on the TCA cycle, thus providing implications for targeted therapy.

44. **Identification of HLA-DR Presented Peptides from Antibiotic-refractory Lyme Arthritis or Rheumatoid Arthritis Patients' Synovia and PBMCs using LC-MS/MS**
Qi Wang1, Elise E. Drouin2, Chunxiang Yao1, Jiyang Zhang3, Yu Huang1, Allen C. Steere2, and Catherine E. Costello1

Introduction: Lyme disease is caused by Borrelia burgdorferi transmitted by tick bites. The cases of Lyme disease with persistent inflammatory arthritis after more than three months of antibiotic treatment are called antibiotic-refractory Lyme arthritis (LA). Rheumatoid arthritis (RA) is an autoimmune disease with chronic inflammatory symptoms in synovial joints similar to antibiotic-refractory LA. In a previous study, we identified ECGF as an autoimmune antigen in some LA patients, which supporting the hypothesis that LA can result in an autoimmune disorder. In this study, HLA-DR-presented peptides were purified from synovial tissue (ST), synovial fluid (SF), or peripheral blood mononuclear cells (PBMC) from patients with LA or RA, and the purified samples were submitted to LC-MS/MS analysis.

Methods: Immunoaffinity purification of HLA-DR-presented peptides was performed from synovial tissue, synovial fluid, or PBMC using a previously published procedure. The eluent from affinity purification was injected into a reversed-phase chromatographic column and CID was used for fragmentation of selected precursor ions. Database searches were conducted with Mascot, OMSSA, and X!Tandem against the Swiss-Prot human database concatenated with a randomized decoy database.

Results: Here, we used LC-MS/MS to identify HLA-DR-presented self-peptides in cells taken directly from clinical samples: ST (N=12), SF (N=6), or PBMC (N=4) from five patients with RA and eight with LA. We identified 1,532 non-redundant HLA-DR-presented peptides, derived from 778 source proteins. As the study progressed, application of newer, higher sensitivity LC-MS/MS instruments increased the number of peptide identifications/sample. Sixty-eight percent of the peptides identified in SFMC and 55% of those found in PBMC were found in ST.

Conclusions: Immunoprecipitation and LC-MS/MS can now identify hundreds of HLA-DR-presented self-peptides from individual patients' tissues or fluids having mixed cell populations. Demonstrated access to HLA-DR-presented peptides from SF or PBMC allows testing of more patients, including those early in the disease. Direct analysis of clinical samples facilitates identification of novel immunogenic T-cell epitopes.

45. Regulation of Tumor Suppressor Genes and DNMT1 in Breast and Ovarian Cancer

Meghan Leary1, Sarah Heerboth1 , Nicole Snyder1, Amber Willbanks1, Karolina Lapinska1, Garrick Horn1, Shannon Byler1, Sibaji Sarkar1,2,3

Epigenetics regulates gene expression through DNA methylation, histone methylation and acetylation, and is associated with a number of diseases. Several types of cancer have been linked to the dysregulation of oncogenes and silencing of tumor suppressor genes. Aberrant silencing of tumor suppressor genes through methylation has been shown to contribute to carcinogenesis. Our laboratory has shown that histone deacetylase inhibitors (HDACi) demethylate and re-express tumor suppressor genes. ARHI is an imprinted pro-apoptotic gene. The maternal allele is silenced by methylation, and the paternal allele is expressed in normal tissues, but is silenced by methylation in breast and ovarian cancer cells, causing loss of heterozygosity (LOH). We hypothesized that re-expression of tumor suppressor genes makes cancer cells susceptible to other drugs. Combination of HDACi and the calpain protease inhibitor calpeptin produced more than additive growth inhibition in breast and ovarian cancer cells. We observed that tumor suppressor genes were demethylated and re-expressed following HDACi treatment. To determine which specific CpG residues were methylated, we sequenced CpG islands in one gene, ARHI. Treatment with HDACi showed differential demethylation in these regions. Demethylation was caused by downregulation of DNMT1. DNMT1 dissociated from HSP90 and HDACi treatment decreased its phosphorylation. We reasoned that some of the demethylated CpG residues regulate the expression of ARHI by the binding of transcription inhibitors, HDAC1 and MBDP2. ChIP analysis revealed that that association of HDAC1 and MBDP2 at the CpG residues decreased after HDACi treatment. These results suggest that HDAC1 and MBDP2 bind to specific methylated regions in the ARHI gene to inhibit transcription. We further hypothesized that epigenetic alterations regulate expression of growth promoting genes by CTCF and the differential expression of epigenetically regulated tumor suppressor genes and growth promoting genes is involved in cancer progenitor cell formation.

46. The BEST-CLI (Best Endovascular versus best Surgical Therapy for patients with Critical Limb Ischemia) Trial promises to establish an evidence –based standard of care in the treatment of patients with CLI

Alik Farber MD, Thomas Cheng MS, Cari Reynolds MPH, Marina Malikova PhD, Kenneth Rosenfield MD, Matthew Menard MD

Background: Critical limb ischemia (CLI) is increasing in prevalence worldwide, and remains a significant source of patient morbidity, mortality and limb loss. At present, the decision to

recommend surgical or endovascular revascularization for patients who are candidates for both varies significantly among providers and is driven more by individual preference than scientific evidence.

Methods and Results: The BEST-CLI Trial is a prospective, randomized, multicenter, multidisciplinary, controlled, superiority trial designed to compare treatment efficacy, functional outcomes, quality of life and cost in patients undergoing best endovascular or best open surgical revascularization. Planned enrollment is 2100 patients who have CLI secondary to infra-inguinal arterial occlusive disease and who are candidates for both treatment options. Approximately 140 clinical sites in the United States and Canada will be participating. A pragmatic trial design requires consensus on patient eligibility by at least two investigators, but leaves the choice of specific procedural strategy within the assigned revascularization approach to the individual treating investigator. Patients with a suitable single segment of greater saphenous vein (SSGSV) available for potential bypass will be randomized into Cohort 1 (n=1620), while patients without a SSGSV will be randomized into Cohort 2 (n=480). The primary efficacy endpoint of the trial is Major Adverse Limb Event (MALE)-Free Survival. Key secondary endpoints include Re-intervention and Amputation-free-survival, Amputation Free-Survival, and MALE-Perioperative Death. The first patient was enrolled at Boston Medical Center in August of 2014. To date, 500 patients have been enrolled at 121 sites.

Conclusions: The BEST-CLI trial is the first randomized controlled trial comparing endovascular therapy to open surgical bypass in patients with CLI to be carried out in North America. This landmark comparative effectiveness trial aims to provide Level I data to clarify the appropriate role for both treatment strategies and help define an evidence-based standard of care for this challenging patient population.

47. Request Not to Publish

48. Protein S-glutathionylation: the Redox Mechanism of Metabolic Stress-induced Endothelial Barrier Dysfunction and Atherosclerosis

Jingyan Han

Background — Protein S-glutathionylation (Pr-SSG), the reversible formation of mixed disulfides between protein cysteinyl thiol groups and glutathione, is the most stable and abundant oxidative modification of proteins, and emerging as a critical redox signaling mechanism in cardiovascular diseases (CVD). However, its role in atherosclerosis (AS), the major cause of CVD, is not known. This study thus aimed to explore the role of Pr-SSG in pathogenesis of AS with specific focus of vascular endothelial barrier dysfunction, an important initiating factor in the development of AS.

Methods and Results: Employing the biotin switch assay, a well-developed approach to assess the level of reversible oxidation of proteins in cells and tissues, we found a marked increase in cysteine oxidation of aortic proteins in whole-tissue lysates of aortas from ApoE-/- mice on Western Diet for 8 weeks, concomitant with significant decrease in reduced form of glutaredoxin-1(Glrx-1), a small cytosolic thiol-transferase that can efficiently and specifically remove the GSH adducts and appears as a pivotal regulator of redox signaling cascades governing a plethora of cellular processes. Pr-SSG in aortic tissue of ApoE-/- mice visualized by immunofluorescence staining with specific antibody against protein-GSH complex, was markedly increased in atherosclerotic lesions. Furthermore, an increased Pr-SSG level was mainly observed in metabolic stressed aortic ECs in vivo and in vitro, which was diminished by up-regulation of Glrx-1 in Glrx TG/ApoE-/- mice and in Glrx adenovirus infected human aortic endothelial cells (HAECs). More importantly, this two-week western diet induced a pro-atherogenic hyper-permeability in aortic endothelium and was prevented in Glrx TG/ ApoE-/- mice without alternation of plasma lipid profiles and proinflammatory responses. Mechanistically, induction of Pr-SSG in aortic endothelium disorganized cytoskeletal actin structure, while up-regulation of Glrx-1 strengthened aortic barrier integrity through activation of small RhoGTPase rac1 and consequent cortical actin formation. Up-regulation of Glrx thus preserve aortic barrier function and alleviate atherosclerotic lesion development.

Conclusions: Pr-SSG in aortic ECs is highly induced by atherogenic stimulus and plays a causative role in aortic barrier dysfunction and development of AS. S-glutathionylation and Glrx-1 are thus positioned as excellent target and bio-therapeutic for cardiovascular injuries associated with oxidative stress, respectively.

49. **Parkinson's and Crohn's disease-associated LRRK2 mutations and LRRK2 inhibitors alter type II interferon responses of human peripheral blood monocyte ex vivo**
Tsuneya Ikezu1,2, Hirohide Asai1, Seiko Ikezu1, Ben Wolozin1,2, Francis Farraye3, and Zbigniew Wszolek4

The Leucine Rich Repeat Kinase 2 (LRRK2) is a causative gene of familial Parkinson's disease (PD). In addition, the M2397 allele of M2397T polymorphism in LRRK2 gene is genetically associated with sporadic Crohn's disease. LRRK2 is highly expressed in neurons in the central nervous system and in human peripheral blood mononuclear cells (PBMCs), especially CD14+ monocytes. Recent studies suggest that LRRK2 transcription is potently induced by type II interferon (IFN-γ and suppresses the activity of the transcription factor Nuclear Factor of Activated T cells (NFAT) in human immune cells. The putative role of LRRK2 in immune function raises the possibility that LRRK2 contributes to PD by altering brain inflammatory response. We hypothesize that IFN-γ induces LRRK2 gene expression, which inhibits NFAT activity, leading to a resolution of IFN-γ-mediated inflammation, and this may be altered in human monocytes

derived from PD or CD patients by LRRK2 mutations. A total of 50 CD and 50 control cases and 15 PD with LRRK2 mutation cases and 20 PD without LRRK2 mutation cases are recruited. We have isolated live CD14+ human monocytes from recruited PD, CD and control cases for ex vivo IFN-γ stimulation. We found that IFN-γ potently enhanced gene expression of pro-inflammatory molecules and LRRK2 itself. Interestingly, specific LRRK2 inhibitors (CZC-25146 and GSK-2578215A) show further enhanced the gene expression, whereas FK506, a NFAT inhibitor, suppressed all the gene induction. M2397 LRRK2 CD risk allele group show enhanced IFN-γ responses in CD but not in control cohort. Monocytes isolated from PD cases with G2019S and R144C LRRK2 mutations show significantly suppressed IFN-γ responses, whereas monocytes from sporadic PD cohort are similar to the ones from control cohort. Interestingly, none of M2397 allele homozygotes are present in the PD cases with G2019S or R144C LRRK2 mutation. These data demonstrate that PD-linked and CD-associated LRRK2 mutations are significant modifiers of innate immune response and potentially important for the immunopathogenesis of PD and CD.

50. Pilot Study of AhR Signaling Components in Breast Cancer Tissue Microarray

Esther Landesman-Bollag, Nathalie Bitar, Carmen Sarita-Reyes, Israa Laklouk, Elizabeth Stanford, Olga Novikov, Zhongyan Wang, Alejandra Ramirez-Cardenas, David Sherr, David C. Seldin

As the age-adjusted incidence of breast cancer has climbed to one in eight women in past decades, it has become critical to identify not only the environmental but also the cellular and molecular pathways responsible for breast cancer formation and progression. Our exposure to more than 80,000 man-made chemicals in the environment, of which fewer than 2% have been evaluated for their carcinogenic potential, could quite possibly contribute to this trend of increased breast cancer susceptibility. A transcription factor that could relay these chemicals' deleterious cellular effects is the aryl hydrocarbon receptor (AhR). The AhR binds to and is activated by (1) environmental carcinogens (xenobiotics) including polycyclic aromatic hydrocarbons, PCBs, and dioxins, and (2) endogenous ligands, such as tryptophan metabolites. Once activated by environmental carcinogens, the AhR initiates aberrant molecular signaling, possibly driving cancer progression and metastasis. In addition, aberrant tryptophan metabolism has long been associated with breast cancer. Dysregulated activation of AhR through endogenous ligands could therefore also contribute to breast carcinogenicity.

In this study, we aim to characterize markers of the AhR pathway by semi-quantifying them in human breast cancer tissue microarray (TMA) FFPE sections using immunohistochemical staining. Components of the AhR pathway that are triggered by xenobiotic and endogenous ligands will be evaluated for subcellular localization, intensity, and distribution in benign epithelium, localized, invasive and metastatic carcinoma, and in stroma (tumor

microenvironment). Components include CYP1B1, a prototypic activated AhR gene target; AhR itself, which is nuclear when active; SOX2, a master regulator of cancer stem cells that we recently showed is a direct downstream target of and is regulated by AhR; ALDH1a3, a marker of cancer stem cells and AhR activity, and TDO2, one of the 2 main enzymes responsible for the catabolism of tryptophan metabolites, and possibly an endogenous driver for a positive feedback loop that may drive breast cancer migration. We will probe correlations between the markers' expression patterns in the TMA, comprised of 50 breast cancer and matched lymph node metastasis carcinoma specimens. Finding correlations linking in vitro data in the AhR pathway in breast cancer cell lines and clinical human samples will provide the translational rationale to explore therapeutic approaches to target the AhR pathway.

51. **"It's all about the label": Understanding the landscape of mental health terminologies in a faith community in Lowell, Massachusetts**

Claire E. Oppenheim1; Lindsey Parnarouskis2, Jeremiah Menyongai3, Bernadette Chukwuezi3, Dorothy Johnson3,Severine P. Kouagheu3,Christiana Onyeulo3, Seide P. Slopadoe3, Peter Wennah3, Gessie Paul3, Jennie B. Morris3,Grace Boykai3,Barbara Jackson3, Nathan Manyika3, Anne Stevenson2, Christina P.C. Borba1,2

Introduction: Approximately one-quarter of residents in Lowell, Massachusetts are foreign born, including many from West Africa and war-affected Liberia and Sierra Leone. While immigrants and especially refugees are at higher risk for mental health problems than the general population, they are less likely to access care. To begin understanding this treatment gap, we explore the community's milieu of mental health terminologies along a spectrum of increasing severity and stigmatization: from emotional health to mental health to craziness.

Methods: In 2014, Massachusetts General Hospital (MGH) Division of Global Psychiatry and the Christ Jubilee International church in Lowell conducted a needs assessment of the health and mental health landscape of this faith community, including an exploration of their use of various mental health terminologies. Data are analyzed from 48 qualitative interviews, conducted by 6 community members trained by the MGH team in research ethics, in-depth interviewing, and study protocol. Data were analyzed by researchers from Boston University (BU) School of Medicine, BU School of Public Health and MGH using thematic analysis in NVivo 11.

Results: Participants described a range of distinct definitions and conceptualizations of emotional health, mental health, and craziness, which were often described as benchmarks along a spectrum of increasing severity. However, participants' descriptions also contained significant overlap and strong associations, such that these distinctions become blurred. Within the sociocultural context of this community, all three interrelated terms carry significant

stigma. Mental health care providers are also stigmatized as seeking these services is perceived as an indication of severe mental illness or "craziness."

Conclusion: Education and awareness are natural antidotes to stigma and were the two most frequently proposed solutions by participants. Future community-based mental health programs must be informed by the community's mental health terminologies and understandings, as well as by the associated climate of stigma.

52. **Triple-negative breast cancers (TNBCs) comprise the most aggressive subtype of breast cancer**
    Fabio Petrocca

In fact, no targeted therapies are currently available against these tumors. Although TNBCs are exceedingly heterogeneous in genetic mutations and copy number variations, they are commonly arrested in a bipotent progenitor epigenetic state. We recently performed a series of siRNA lethality screens to identify, in an unbiased way, recurrent TNBC vulnerabilities linked to this phenotype. The screens re-discovered mitosis as a frequent Achilles' heel of these tumors (antimitotic drugs are currently a mainstay of TNBC therapy). Top hits were also highly enriched for proteasome subunits and a subset of proteins comprising the so-called tri-snRNP spliceosome complex, which orchestrates a specific step in the RNA splicing pathway. Although RNA splicing is critical for the maturation, and therefore the expression, of virtually all human transcripts, it is becoming apparent that the system is quite redundant and that individual splicing factors may in fact be essential for the processing of limited sets of genes. In fact, we found that silencing individual tri-snRNP proteins by RNAi only affected the expression of ~ 30 genes in TNBC cells. Amongst these, Mcl-1 stood out as an interesting candidate to explain TNBC selective dependency, since we previously showed that these tumors are exquisitely addicted to Mcl-1 for survival. Together, our data suggest that targeting the tri-snRNP complex might be a *broad-spectrum* strategy to tackle TNBCs driven by diverse genetic lesions. Of note, the tri-snRNP complex is also emerging as an attractive therapeutic node in colorectal cancer and multiple myeloma. However, selective tri-snRNP inhibitors to systematically probe the therapeutic potential of these findings in vivo are not available. We recently launched a drug discovery campaign to develop the first generation of such inhibitors.

53. **Opioid analgesia use after ambulatory surgery: mismatch between quantities prescribed and used**
    Christopher Shanahan, MD MPH; Inga Holmdahl, BA; Olivia Gamble, BA; Julia Keosaian, MPH; Ziming Xuan ScD; Jane Liebschutz, MD MPH

Abstract: Opioid prescriptions for post-operative pain have been implicated in steering patients toward addiction, or, conversely, are overprescribed and can lead to opioid diversion. We aimed to characterize surgeons' post-operative opioid analgesia prescribing practices and

patient experiences through a prospective study of patients undergoing elective ambulatory surgery. We surveyed patients longitudinally 1 week prior to and 1 week after planned ambulatory surgery at an academic safety-net hospital. Surgery types chosen for this study were considered by surgeons to be painful enough in the post-operative period to require opioid pain medications. Specialties performing these surgeries included orthopedic, otolaryngology, general, podiatry, maxillofacial, gynecology, and urology. Patients were recruited and interviewed in-person at pre-operative appointments or via mailed personalized letter (with an opt-out option) followed by a phone call. One to fourteen days prior to surgery, Patients were administered a baseline questionnaire, covering socio-demographics, pain severity and disability (Graded Chronic Pain Scale), as well as alcohol and drug use disorders (AUDIT and DUDIT). Follow-up assessment at 10-14 days post-operatively via telephone included assessment of post-operative pain (International Pain Outcomes questionnaire), validated scales to identify opioid medication misuse (the POMI and PMQ), and questions about prescription medication disposal and storage. We obtained follow-up data from 149 Patients (83% retention rate), of which 53% were female and the mean age was 49. The 18 surgeons who cared for the 149 Patients prescribed opioid medications for post-operative analgesia to 141 (95%). Of those 141 Patients, 128 (91%) were prescribed a medication containing oxycodone. Surgeons prescribed 4840 pills total (avg. 33 pills). PTs reported taking only 1961 of those prescribed pills (42%, avg. 15 pills) over the 10-day post-operative period. At follow-up, using a 0-10 scale, 32% of participants rated their pain relief effectiveness as “Complete” (10), 36% “High” (7-9), 24% “Moderate” (4-6), 5% “Low” (1-3), and 3% “Ineffective” (0). Of those Patients taking opioid pain medications, 18 (14%) reported taking them more often than prescribed and 13 (10%) reported seeking an early refill. The majority of Patients (n=106; 71%) reported having leftover medication and when ask how they planned to handle these pills, of whom 37 (35%) reported intent to dispose of them safely (flushing or giving to police), 37 (35%) planned to keep them, 17 (16%) planned to continue taking them, and 15 (14%) did not respond to this question. For elective ambulatory procedures, most participants reported using significantly less post-operative opioid pain medication than prescribed. Nearly half of participants reported plans to retain unused medications after pain resolution. To reduce unnecessary opioid prescribing and potential availability for diversion and misuse, improved prescribing and disposal practices are needed.

54. “Never Events” After Vascular Surgery Procedures

Jeffrey Siracuse

Objectives: Never Events refer to harmful hospital acquired conditions that the Centers for Medicare and Medicaid Services (CMS) identified in 2008 as largely preventable and that would no longer be reimbursed. Our goal was to identify the incidence, predictive factors, temporal

trend, and associated consequences of never events after major open vascular surgery procedures.

Methods: The National (Nationwide) Inpatient Sample (2003-2011) was queried to identify Never Events applicable to vascular surgery patients including air embolism, catheter based urinary tract infections (UTI), stage 3 and 4 pressure ulcers, falls/trauma, blood incompatibility, vascular catheter infections, complications of poor glucose control, retained foreign objects, and wrong site surgery. We specifically evaluated open abdominal aortic aneurysm (AAA) repair, carotid endarterectomy (CEA), and lower extremity bypass/femoral endarterectomy (LEB). Multivariable logistic regression was used to predict Never Events based on preoperative variables. Multivariable logistic and gamma regression models were used to study mortality, hospital length of stay (LOS), and charges.

Results: There were 774 patients with Never Events identified among 267,734 patients. The distribution of Never Events were as follows: Falls/trauma (59%), pressure ulcers (19%), catheter based UTI (9%), vascular catheter infection (6%), complications of poor glucose control (5%), and retained objects (4%). Rates of falls and catheter based UTIs have increased since 2008. Multivariable predictors of any Never Event included LEB, AAA, weight loss, non-elective admission, paralysis, repair, congestive heart failure, altered mental status, renal failure, weekend admission, diabetes, female gender, and age. Race, insurance, hospital type, income level, geography, July to September admission, and other comorbidities were not predictive. After risk factor adjustment, never events were associated with increased perioperative mortality (OR 2.7, 95% CI 1.5-34.8, P<.001), LOS (Means Ratio (MR) 1.9, 95% CI 1.7-2.0, P<.001), and total charges (MR 1.7, 95% CI 1.6-1.8, P<.001).

Conclusion: Never Events after major vascular surgery are associated with a number of perioperative factors and are predictive of increased charges, LOS, and mortality. Falls and catheter based UTIs have increased in frequency since CMS announced that it would no longer reimburse for these complications. This study establishes baseline Never Event rates in the vascular surgery patient population and identifies high-risk patients to target for quality improvement.

55. Screening tetracycline analogs to disrupt light chain amyloid fibrils

Jennifer E. Ward1, 2, Varuna Shibad1,2, Michael Greene2, Lawreen H. Connors2 and David C. Seldin1,2

Introduction: Tetracycline and some of its derivatives are capable of disrupting amyloid fibrils (1-3). We demonstrated that doxycycline could disrupt purified and recombinant immunoglobulin light chain fibrils in vitro and prevent amyloid formation in vivo in a transgenic

mouse model of AL amyloidosis (4). Multiple centers, including BU, are evaluating the effectiveness of doxycycline in systemic amyloidosis patients. We tested the ability of other tetracycline analogs to disrupt amyloid fibrils, to identify drugs with increased anti-fibril activity and potentially fewer side effects.

Methods: Ex vivo fibrils from water wash tissue extractions suspended in phosphate-buffered saline were incubated with tetracycline analogs at multiple doses for 3-7 days. Fibril disruption was measured by changes in turbidity and imaged by negative stain electron microscopy. The possibility that the disrupted products formed cytotoxic oligomers was examined by measuring the viability of SH-SY5Y neuroblastoma and H9C2 cardiomyoblast cells incubated with drug-treated fibrils.

Results: Eight commercially available tetracycline antibiotics (tetracycline, doxycycline, minocycline, rolitetracycline, methacycline, oxytetracycline, 4-epitetracycline, meclocycline) and one novel compound were found to increase turbidity of suspensions of fibrils at wavelengths >500 nm. The dissociated protein products of these reactions demonstrated loss of typical 10 nm fibril structure by electron microscopy; aggregated and clumped proteins were seen and were not cytotoxic to cardiomyocyte or neuronal cell lines.

Conclusions: Minocycline and methacycline may disrupt amyloid fibrils in vitro more effectively than doxycycline or tetracycline. Doxycycline and tetracycline disrupt amyloid fibrils in vitro in a dose dependent manner. Due to adverse effects of long term antibiotic therapy, the effectiveness of lower doses of doxycycline should be tested in the AL amyloidosis transgenic mouse model. Novel analogs which retain the ability to disrupt amyloid fibrils with potentially less adverse side effects are a goal of future studies.

56. **Identification of Pseudolysin (lasB) as a Gluten-Degrading Enzyme with Therapeutic Potential for Celiac Disease**
    Guoxian Wei 1, Na Tian1, Adriana C Valery1, Yi Zhong1, Detlef Schuppan 2, 3 and Eva J Helmerhorst1

Objectives: Immunogenic gluten proteins implicated in celiac disease (CD) largely resist degradation by human digestive enzymes. Here we pursued the isolation of gluten-degrading organisms from human feces, aiming at bacteria that would digest gluten under acidic conditions, as prevails in the stomach.

Methods: Bacteria with gluten-degrading activities were isolated using selective gluten agar plates at pH 4.0 and 7.0. Proteins in concentrated bacterial cell sonicates were separated by diethylaminoethanol chromatography. Enzyme activity was monitored with chromogenic

substrates and gliadin zymography. Elimination of major immunogenic gluten epitopes was studied with R5 and G12 enzyme-linked immunosorbent assays.

Results: Gliadin-degrading enzyme activities were observed for 43 fecal isolates, displaying activities in the ~150–200 and <50 kDa regions. The active strains were identified as Pseudomonas aeruginosa. Gliadin degradation in gel was observed from pH 2.0 to 7.0. Liquid chromatography–electrospray ionization–tandem mass spectrometry analysis identified the enzyme as pseudolysin (lasB), a metalloprotease belonging to the thermolysin (M4) family proteases. Its electrophoretic mobility in SDS–polyacrylamide gel electrophoresis and gliadin zymogram gels was similar to that of a commercial lasB preparation, with tendency of oligomerization. Pseudolysin eliminated epitopes recognized by the R5 antibody, while those detected by the G12 antibody remained intact, despite destruction of the nearby major T-cell epitope QPQLPY.

Conclusions: Pseudolysin was identified as an enzyme cleaving gluten effectively at extremely low as well as near-neutral pH values. The potential to degrade gluten during gastric transport opens possibilities for its application as a novel therapeutic agent for the treatment of CD.

57. **C2 domain-containing protein CDP138 plays an important role in energy balance and fat browning through regulating adrenaline release**
    Qiong L. Zhou, Ye Song, Boris Jun-Yuan Huang, Andria G. Sharma, Kavin Zhu, Zhangping Liao, and Zhen Y. Jiang

CDP138 is a calcium- and lipid-binding protein that is known to be involved in membrane trafficking. Here we report that mice without CDP138 develop obesity under both a normal chow diet (NCD) and a high fat diet (HFD) conditions. CDP138-/- mice have lower energy expenditure, oxygen consumption and body temperature in comparison with Wild-Type (WT) mice. Interestingly, CDP138 is highly expressed in the medulla, but not cortex, of the adrenal grand and is required for cold exposure-induced adrenaline secretion into the circulation. In addition, tissue cyclic adenosine monophosphate (cAMP) levels, hormone sensitive lipase (HSL) phosphorylation, and adipose triglyceride lipase (ATGL) protein expression were decreased in CDP138-/- mice. Furthermore, thermogenesis and inguinal fat browning in cold condition were also decreased in CDP138-/- mice. Our data indicate that CDP138 is a novel regulator of acute stress response and plays an important role in lipid metabolism through regulating adrenaline secretion from adrenal grand.

Dissecting the regulatory roles of the MEF2 transcription factors in cardiac muscle